

การสกัดด้วยเฟสของแข็งแบบออนไลน์ร่วมกับระบบซีเคิร์นเซียมอินเจกชัน
สำหรับตรวจวัดซัลโฟนาไมด์

นางสาว พิมพัชวิญ จันทระ

วิทยานิพนธ์นี้เป็นส่วนหนึ่งของการศึกษาตามหลักสูตรปริญญาวิทยาศาสตรมหาบัณฑิต
สาขาวิชาเทคโนโลยีชีวภาพ
คณะวิทยาศาสตร์ จุฬาลงกรณ์มหาวิทยาลัย
ปีการศึกษา 2552
ลิขสิทธิ์ของจุฬาลงกรณ์มหาวิทยาลัย

ON-LINE SOLID PHASE EXTRACTION COUPLED WITH SEQUENTIAL
INJECTION SYSTEM FOR DETERMINATION OF SULFONAMIDES

Miss Pimkwan Chantarateepa

A Thesis Submitted in Partial Fulfillment of the Requirements
for the Degree of Master of Science Program in Biotechnology

Faculty of Science

Chulalongkorn University

Academic Year 2009

Copyright of Chulalongkorn University

พิมพ์ขวัญ จันทรทีประ : การสกัดด้วยเฟสของแข็งแบบออนไลน์ร่วมกับระบบ
 ซีเควินเซ็ลอินเจ็คชันสำหรับตรวจวัดซัลโฟนาไมด์ (ON-LINE SOLID PHASE
 EXTRACTION COUPLED WITH SEQUENTIAL INJECTION SYSTEM FOR
 DETERMINATION OF SULFONAMIDES) อ.ที่ปรึกษาวิทยานิพนธ์หลัก : รศ. ดร.
 อรรวรรณ ชัยลภากุล, 90 หน้า.

ในงานวิจัยนี้ได้พัฒนาการแยกและวิเคราะห์เชิงปริมาณของซัลโฟนาไมด์ โดยใช้
 วิธีการสกัดด้วยเฟสของแข็งแบบออนไลน์ ร่วมกับเทคนิคซีเควินเซ็ลอินเจ็คชันอะนาไลซิส สำหรับ
 กระบวนการการสกัดด้วยเฟสของแข็ง จะมีคอลัมน์ขนาดเล็กซึ่งทำขึ้นเอง ภายในบรรจุด้วยอนุภาค
 ของตัวดูดซับ กระบวนการนี้จะเป็นอัตโนมัติทั้งในการกำจัดสิ่งเจือปนออกจากตัวอย่างและการ
 สกัด ซึ่งกระบวนการนี้จะต่อกับระบบซีเควินเซ็ลอินเจ็คชันอะนาไลซิส โดยที่ระบบนี้จะประกอบ
 ไปด้วย ปุ่มสำหรับควบคุมการไหลและวาล์ว วิธีนี้สามารถที่จะทำได้อย่างต่อเนื่องตั้งแต่การ
 สกัดซัลโฟนาไมด์จากตัวอย่างที่เป็นของเหลว ไปจนถึงการแยกสารที่สนใจโดยใช้เทคนิคไฮเพอร์
 ฟอรัแมนซ์ลิควิดโครมาโทกราฟี ร่วมกับการตรวจวัดทางเคมีไฟฟ้า งานวิจัยนี้ได้ศึกษาหาภาวะที่
 เหมาะสมของการสกัดด้วยเฟสของแข็งแบบออนไลน์ ได้แก่ ศึกษาหาอัตราส่วนที่เหมาะสมของ
 สารที่ใช้เป็นตัวชะ, อัตราการไหลของสารในขั้นตอนการผ่านสารตัวอย่างและการชะสารตัวอย่าง
 และ โชนของสารที่ถูกชะออกมา จากการศึกษาพบว่า อัตราส่วนที่เหมาะสมของสารที่ใช้ชะคือ
 เมทานอลต่อเฟสเคลื่อนที่ 100:0, อัตราการไหลของสารในขั้นตอนการผ่านสารตัวอย่างและการชะ
 สารตัวอย่างที่เหมาะสมคือ 10 ไมโครลิตรต่อวินาที และ โชนของสารที่ถูกชะที่เหมาะสมคือ 20-24
 วินาที ความสัมพันธ์ระหว่างพื้นที่ของพีกกับความเข้มข้นของสารซัลโฟนาไมด์เป็นเส้นตรงในช่วง
 0.01-8 ส่วนในล้านส่วน จากผลการทดลองชี้ให้เห็นว่า วิธีนี้เป็นวิธีที่ง่าย, รวดเร็ว และมีความไวสูง
 สำหรับการแยกและวิเคราะห์เชิงปริมาณของสารซัลโฟนาไมด์

สาขาวิชา.....เทคโนโลยีชีวภาพ..... ลายมือชื่อนิสิต.....
 ปีการศึกษา.....2552..... ลายมือชื่อ อ.ที่ปรึกษาวิทยานิพนธ์หลัก.....

4972592023 : MAJOR BIOTECHNOLOGY

KEYWORDS : SULFONAMIDE/ SEQUENTIAL-INJECTION ANALYSIS/ ON-LINE SOLID-PHASE EXTRACTION/ AMPEROMETRY/ BORON-DOPED DIAMOND ELECTRODE

PIMKWAN CHANTARATEEPRA : ON-LINE SOLID PHASE EXTRACTION COUPLED WITH SEQUENTIAL INJECTION SYSTEM FOR DETERMINATION OF SULFONAMIDES. THESIS ADVISOR : ASSOC. PROF. ORAWON CHAILAPAKUL, Ph.D., 90 pp.

In this work, sequential-injection on-line solid-phase extraction (SPE) coupled with high-performance liquid chromatography (HPLC) for the separation and determination of sulfonamides (SAs) has been developed. A homemade microcolumn SPE was automated by sequential-injection analysis to perform on-line sample clean-up and extraction. A sequential-injection analysis (SIA) system consisting of a syringe pump and multi-position valve was constructed. This method can continuously extract sulfonamides from aqueous samples followed by the separation of sulfonamides using HPLC coupled with boron-doped diamond (BDD) electrode as electrochemical detection. The conditions for on-line SPE including eluent, flow rate of sample loading and elution, and zone of eluate were investigated. An eluent composition of methanol was selected. The optimal flow rate of sample loading and elution was found to be 10 $\mu\text{L/s}$ and optimal elution time was 20-24 s. Under optimal conditions, a linear relationship between peak height and sulfonamides concentration was obtained in the range of 0.01-8 ppm. The results demonstrate that this method is simple, rapid and highly sensitive for the automated extraction, separation, and determination of sulfonamides.

Field of Study :.....Biotechnology..... Student's Signature.....

Academic Year :..... 2009..... Advisor's Signature.....

ACKNOWLEDGEMENTS

First of all, I would like to thank my thesis advisor, Associate Professor Dr. Orawon Chailapakul for her invaluable guidance, kind advice and encouragement. Furthermore, I would also like to thank other members of the thesis committee for their extensive and excellent comments on early works and drafts of the thesis.

This research was financially supported by Innovation for the improvement of food safety and food quality for new world economy project, The 90TH Anniversary of Chulalongkorn University Fund, and Center of Excellence for Petroleum, Petrochemicals and Advanced Materials, Chulalongkorn University.

Special thanks go to all members of the electrochemical research group, Chulalongkorn University for wonderful friendship, suggestion and encouragement.

Finally, I would like to express my deepest gratitude and sincerest thank to my family for understanding and encouragement throughout the retire course of study.

CONTENTS

	page
ABSTRACT (THAI).....	iv
ABSTRACT (ENGLISH).....	v
ACKNOWLEDGEMENTS.....	vi
CONTENTS.....	vii
LIST OF TABLES.....	xii
LIST OF FIGURES.....	xiii
LIST OF ABBREVIATIONS.....	xvii
CHAPTER I INTRODUCTION.....	1
1.1 Introduction and literature reviews.....	1
1.2 Research objectives.....	3
1.3 Scope of research.....	3
CHAPTER II THEORY	4
2.1 Flow-Analysis Techniques.....	4
2.1.1 Flow Injection Analysis	4
2.1.2 Sequential Injection Analysis.....	5
2.2 High Performance Liquid Chromatography (HPLC).....	7
2.2.1 High Performance Adsorption Chromatography.....	10
2.2.2 Instrumentation.....	10
2.2.2.1 Mobile Phase Reservoir	11
2.2.2.2 Pump.....	11
2.2.2.3 Injector.....	12
2.2.2.4 Columns.....	12
2.2.2.5 Silica-Based Monolithic Columns	14

	page
2.2.2.5.1 Formation Processes and Pore Structure Control of Silica Monoliths.....	14
2.2.2.6 Detectors.....	17
2.3 Fundamental of Electrochemistry.....	18
2.3.1 Mass transport	19
2.3.1.1 Diffusion	19
2.3.1.2 Migration	19
2.3.1.3 Convection	19
2.3.2 Voltammetry.....	20
2.3.3 Cyclic Voltammetry.....	22
2.3.4 Amperometry.....	25
2.3.5 Working electrode	26
2.3.5.1 Boron-doped diamond (BDD).....	26
2.3.6 Flow Cell for Electrochemistry	29
2.4 Sample Preparation.....	30
2.4.1 Solid-Phase Extraction (SPE).....	31
2.4.1.1 Mode of solid-phase extraction	32
2.4.1.1.1 Reversed phase.....	32
2.4.1.1.2 Normal phase.....	32
2.4.1.1.3 Ion exchange.....	32
2.4.1.1.4 Mixed mode.....	33
2.4.1.2 Step of solid phase extraction.....	34

	page
CHAPTER III EXPERIMENTAL	37
3.1 Chemical and Reagents	37
3.2 Instruments and Equipment	37
3.3 Preparation of solutions	39
3.3.1 Preparation of solution in Cyclic Voltammetry.....	39
3.3.1.1 Standard Stock Solutions.....	39
3.3.1.2 Supporting Electrolyte.....	39
3.3.1.3 Working Standard Solution.....	39
3.3.2 Preparation of solution for HPLC-EC.....	40
3.3.2.1 Standard Stock Solution.....	40
3.3.2.2 Mobile phase.....	40
3.3.3 Preparation of solution for Sample Preparation.....	41
3.3.3.1 Na ₂ EDTA-MacIlvaine's Buffer Solution	41
3.3.4 Preparation of SPE column.....	41
3.3.5 Preparation of Sample.....	42
3.4 Procedure.....	42
3.4.1 Cyclic Voltammetry.....	42
3.4.1.1 The Scan Rate Dependence Study.....	43
3.4.1.2 The Concentration Dependence Study.....	44
3.4.2 On-line SPE-HPLC procedure.....	44
3.4.2.1 Effect of eluent.....	48
3.4.2.2 Effect of sample loading and eluting rate.....	48
3.4.2.3 Effect of eluate zone.....	48

	page
3.4.2.4 Linearity.....	48
3.4.2.5 Limit of Detection (LOD) and Limit of Quantitation (LOQ).....	48
3.4.2.6 Precision and Accuracy.....	49
3.4.2.7 Comparison of Methods between the HPLC-EC and HPLC-MS.....	49
CHAPTER IV RESULTS AND DISCUSSIONS.....	50
4.1 Cyclic Voltammetric Investigation.....	50
4.1.1 The Scan Rate Dependence Study.....	52
4.1.2 The Concentration Dependence Study.....	60
4.2 Optimal Conditions of HPLC-EC	66
4.3 On-line SPE-HPLC-EC.....	67
4.3.1 Effect of eluent.....	67
4.3.2 Effect of sample loading and eluting rate.....	68
4.3.3 Effect of eluate zone.....	69
4.3.4 Calibration and linearity.....	70
4.3.5 LOD and LOQ.....	73
4.4 Application to Real Sample.....	73
4.4.1 Determination of SAs in shrimp.....	73
4.4.2 Accuracy and Precision.....	75
4.4.3 Comparison of Methods between the HPLC-EC and HPLC-MS...	78
CHAPTER V CONCLUSION AND FUTURE PERSPECTIVES	79
REFERENCES.....	81

	page
APPENDIX	87
VITAE	102

LIST OF TABLES

Table		page
2.1	Comparison between SIA and FIA	6
3.1	Composition of each concentration for seven sulfonamides in electrochemical cell for cyclic voltammetry.....	40
3.1	List of chemicals and their suppliers.....	34
3.2	The SIA operating sequence for sulfonamides analysis.....	47
3.3	The HPLC-EC conditions for the detection of seven SAs.....	47
4.1	Potential of 0.1 mM SAs in 0.05 M phosphate solution pH 3.0, scan rate 50 mV s ⁻¹ at BDD electrode.....	52
4.2	Linearity, limit of detection and limit of quantitation of the method.	71
4.3	LOD and LOQ of seven standard SAs.....	73
4.4	Intra-day precisions and recoveries of spiked level 2, 4, and 6 µg mL ⁻¹	76
4.5	Inter-day precisions and recoveries of spiked level 2, 4, and 6 µg mL ⁻¹	77
4.6	Comparisons results of two methods in shrimp sample.....	78

LIST OF FIGURES

Figure	page
1.1 Chemical structures of the studied sulfonamides.....	2
2.1 A typical manifold of flow injection analysis.....	5
2.2 A typical manifold of sequential injection analysis.....	5
2.3 Potential of SIA for automated sample pre-treatment	7
2.4 Types of liquid chromatography	8
2.5 Schematic representation of the four modes of liquid chromatography.....	9
2.6 Components of a typical HPLC instrument.....	10
2.7 Schematic diagram of a loop injector in the (A) load and (B) inject positions.....	13
2.8 Reaction of bonded stationary phase.....	14
2.9 (A) Nucleation and growth (diffusion limited) of silica-based monoliths (B) Spinodal decomposition (spontaneous) of silica-based monoliths.....	16
2.10 SEM photographs for the bimodal pore structure of silica-based monolithic column.....	17
2.11 Typical excitation signals for voltammetry.....	22
2.12 Cyclic voltammetry waveform.....	23
2.13 Typical cyclic voltammogram where i_{pc} and i_{pa} show the peak cathodic and anodic current respectively for a reversible reaction.....	24
2.14 A typical waveform in amperometry.....	25
2.15 Cyclic voltammetric for diamond in 0.1 M H ₂ SO ₄ . The range of potential windows for glassy carbon and Hg electrodes are shown for comparison.....	27
2.16 SEM image of a boron-doped crystalline diamond.....	28
2.17 Block diagram of a typical microwave plasma CVD reactor	29
2.18 Schematic diagram of thin-layer amperometric flow cell.....	30

Figure	page
2.19 Anatomy of a cartridge SPE.....	31
2.20 Mixed-mode SPE.....	33
2.21 Structure of Oasis HLB cartridges.....	34
2.22 Step of solid-phase extraction.....	36
3.1 The preparation of SPE microcolumn.....	42
3.2 The electrochemical cell for cyclic voltammetry experiment	43
3.3 The manifold diagram of on-line SPE-HPLC system. SP, Syringe pump; SL, Selection valve; SW, Switching valve; HC, Holding coil; L, Loop; SPE, Solid phase extraction.....	44
3.4 Monolithic column silica base.....	45
3.5 A thin-layer flow cell.....	45
3.6 The on-line SPE-HPLC-EC system	46
4.1 Cyclic voltammograms for 0.1 mM standard solutions of SQ, SDM, SDZ, SG, SMM, SMX and SMZ in phosphate buffer solution (pH 3) at BDD electrode. The scan rate was 50 mV s ⁻¹	51
4.2 Cyclic voltammograms for 0.5 mM SQ in phosphate buffer solution (pH 3) at BDD electrode. The scan rate was varied from 10 to 200 mV s ⁻¹ . Inset shows the relationship of the current response versus the square root of the scan rate (v ^{1/2}).....	53
4.3 Cyclic voltammograms for 0.5 mM SDZ in phosphate buffer solution (pH 3) at BDD electrode. The scan rate was varied from 10 to 200 mV s ⁻¹ . Inset shows the relationship of the current response versus the square root of the scan rate (v ^{1/2}).....	54
4.4 Cyclic voltammograms for 0.5 mM SMZ in phosphate buffer solution (pH 3) at BDD electrode. The scan rate was varied from 10 to 200 mV s ⁻¹ . Inset shows the relationship of the current response versus the square root of the scan rate (v ^{1/2}).....	55

Figure	page
4.5 Cyclic voltammograms for 0.5 mM SMM in phosphate buffer solution (pH 3) at BDD electrode. The scan rate was varied from 10 to 200 mV s ⁻¹ . Inset shows the relationship of the current response versus the square root of the scan rate (v ^{1/2}).....	56
4.6 Cyclic voltammograms for 0.5 mM SMX in phosphate buffer solution (pH 3) at BDD electrode. The scan rate was varied from 10 to 200 mV s ⁻¹ . Inset shows the relationship of the current response versus the square root of the scan rate (v ^{1/2}).....	57
4.7 Cyclic voltammograms for 0.5 mM SDM in phosphate buffer solution (pH 3) at BDD electrode. The scan rate was varied from 10 to 200 mV s ⁻¹ . Inset shows the relationship of the current response versus the square root of the scan rate (v ^{1/2})	58
4.8 Cyclic voltammograms for 0.5 mM SQ in phosphate buffer solution (pH 3) at BDD electrode. The scan rate was varied from 10 to 200 mV s ⁻¹ . Inset shows the relationship of the current response versus the square root of the scan rate (v ^{1/2}).....	59
4.9 Cyclic voltammograms of SG in phosphate buffer solution (pH 3) at BDD electrode. The concentration was increased from 0.1 to 1 mM. Inset shows the relationship of the current response against the concentration.....	60
4.10 Cyclic voltammograms of SDZ in phosphate buffer solution (pH 3) at BDD electrode. The concentration was increased from 0.1 to 1 mM. Inset shows the relationship of the current response against the concentration.....	61
4.11 Cyclic voltammograms of SMZ in phosphate buffer solution (pH 3) at BDD electrode. The concentration was increased from 0.1 to 1 mM. Inset shows the relationship of the current response against the concentration.....	62

Figure	page
4.12 Cyclic voltammograms of SMM in phosphate buffer solution (pH 3) at BDD electrode. The concentration was increased from 0.1 to 1 mM. Inset shows the relationship of the current response against the concentration.....	63
4.13 Cyclic voltammograms of SMX in phosphate buffer solution (pH 3) at BDD electrode. The concentration was increased from 0.1 to 1 mM. Inset shows the relationship of the current response against the concentration.....	64
4.14 Cyclic voltammograms of SDM in phosphate buffer solution (pH 3) at BDD electrode. The concentration was increased from 0.1 to 1 mM. Inset shows the relationship of the current response against the concentration.....	65
4.15 Cyclic voltammograms of SQ in phosphate buffer solution (pH 3) at BDD electrode. The concentration was increased from 0.1 to 1 mM. Inset shows the relationship of the current response against the concentration.....	66
4.16 HPLC-EC chromatogram of a 10 $\mu\text{g mL}^{-1}$ mixture of seven standard SAs separated on a monolithic column at flow rate 1.5 mL min^{-1} . The detection potential was 1.2 V vs. Ag/AgCl using a BDD electrode.....	67
4.17 HPLC chromatograms of sulfonamides (10 $\mu\text{g mL}^{-1}$) at different ratio of methanol and mobile phase. (a) methanol, (b) methanol and mobile phase 90:10, (c) methanol and mobile phase 80:20, (d) methanol and mobile phase 70:30, (e) methanol and mobile phase 60:40, (f) methanol and mobile phase 50:50.....	68
4.18 HPLC chromatograms of seven sulfonamides (10 $\mu\text{g mL}^{-1}$) at different sample loading flow rates and eluting flow rate. (1) sulfaguanidine, (2) sulfadiazine, (3) sulfamethazine, (4) sulfamonomethoxine, (5) sulfamethoxazole, (6) sulfadimethoxine, (7) sulfaquinoxaline.....	69

Figure		page
4.19	HPLC chromatograms of sulfonamides at different zone of eluate. (a) zone of eluate at time 20-24 s, (b) zone of eluate at time 25-29 s, (c) zone of eluate at time 30-34 s.....	70
4.20	Linearity of seven standard SAs by HPLC-EC using BDD electrode.....	72
4.21	HPLC-EC chromatogram of (A) a shrimp sample spiked with 6 $\mu\text{g mL}^{-1}$ of standard mixture of seven SAs; (B) a blank shrimp sample separated on a monolithic column at flow rate 1.5 mL min^{-1} . The detection potential was 1.2 V vs. Ag/AgCl using a BDD electrode...	74

LIST OF ABBREVIATIONS

BDD	Boron-doped diamond electrode
CE	Capillary electrophoresis
CV	Cyclic voltammetry
°C	Degree celsius
E	Potential
E^0	Formal reduction potential
$E_{1/2}$	Half-wave potential
EC	Electrochemical
ELISA	Enzyme-linked immunosorbent assay
E_{pa}	Anodic peak potential
E_{pc}	Cathodic peak potential
EU	European Union
FIA	Flow injection analysis
SIA	Sequential injection analysis
HPLC	High performance chromatography
L	Liter
LLE	Liquid-liquid extraction
SPE	Solid-phase extraction
MSPD	Matrix solid-phase dispersion
M	Molar
mL	Milliliter
min	Minute
MRL	Maximum residue limit
MS	Mass spectrometry
n	Number of electron
I	Current
I_p	Peak current
R^2	Correlation coefficient
SA	Sulfonamide
S/B	Signal to background ratio
SDM	Sulfadimethoxine

SDZ	Sulfadiazine
SG	Sulfaguanidine
SMM	Sulfamonomethoxin
SMX	Sulfamethoxazole
SMZ	Sulfamethazine
SQ	Sulfaquinoxaline
T	Time
TLC	Thin-layer chromatography
V	Volt
v/v	Volume by volume
μA	Microampere
μL	Microliter
v	Scan rate

CHAPTER I

INTRODUCTION

1.1 Introduction

Sulfonamides are among the most widely used antibacterial agents because of their low cost, low toxicity, and excellent activity against common bacterial diseases [1-2]. They are used for therapy, prophylaxis, and growth promotion in livestock. However, long-term use of sulfonamide agents can cause serious side effects, such as Stevens-Johnson syndrome and carcinogenicity because of human consumption [3-4]. Additionally antibacterial drug in food can cause anaphylaxis in sensitive patients and can foster the development of antibiotic resistance in pathogenic organisms. The European Union (EU) has set the maximum residual level of sulfonamides in edible tissues and in milk at 100 ng/g [5]. Several conventional methods for the separation and determination of the sulfonamide content of different samples have been reported: gas chromatography (GC), gas chromatography-mass spectrometry (GC/MS), capillary electrophoresis (CE) [6-7], enzyme-linked immunosorbent assay (ELISA) [8], thin-layer chromatography (TLC), high-performance liquid chromatography–mass spectrometry (HPLC/MS), and high-performance liquid chromatography (HPLC) [9-16]. The common detectors used in the analysis of sulfonamides are ultraviolet (UV) [17-24] and fluorescence [1, 25], which exhibit high sensitivity and selectivity. Even though these methods provide high sensitivity and selectivity, these equipments need laboratory space to house them. They are also expensive. Moreover, they still require sample preparation, such as solid phase extraction (SPE) [1, 9, 11-14, 23] or liquid phase extraction (LPE) [21,26] that significantly increase analysis time. Nowadays, HPLC coupled with on-line solid phase extraction (SPE) has been reported [27-32] to significantly improve this problem. On-line SPE is an attractive sample preparation technique because it can reduce sample preparation time and increase sample throughput [16]. Sequential injection analysis (SIA) is a suitable technique for on-line SPE and can be coupled with electrochemical detection (EC). Electrochemical detection not only utilizes low cost instrumentation, but it is also fast and highly sensitive [26,33]. Of the SPE materials that have been reported in the

literature, Oasis HLB was the most attractive for this study. This material is a hydrophilic-lipophilic balanced (HLB) sorbent in SPE that is composed of two monomers (N-vinylpyrrolidone and divinylbenzene). This material exhibited excellent retention capacity for a wide polarity of analytes in previous studies [9,15].

In this work, the aim was to develop on-line SPE techniques coupled with sequential injection analysis for the separation and determination of seven sulfonamides-sulfaguanidine (SG), sulfadiazine (SDZ), sulfamethazine (SMZ), sulfamonomethoxine (SMM), sulfamethoxazole (SMX), sulfadimethoxine (SDM), and sulfaquinoxaline (SQ)-by HPLC using electrochemical detection. A silica-based monolithic column was employed for sulfonamide separation because of its high tolerance for organic solvent, which led to a longer lifetime, and lower backpressure, relative to traditional columns. This methodology was then applied to determine residual concentrations of the seven sulfonamides (Figure 1.1) in shrimp using the Oasis HLB SPE material for sample extraction.

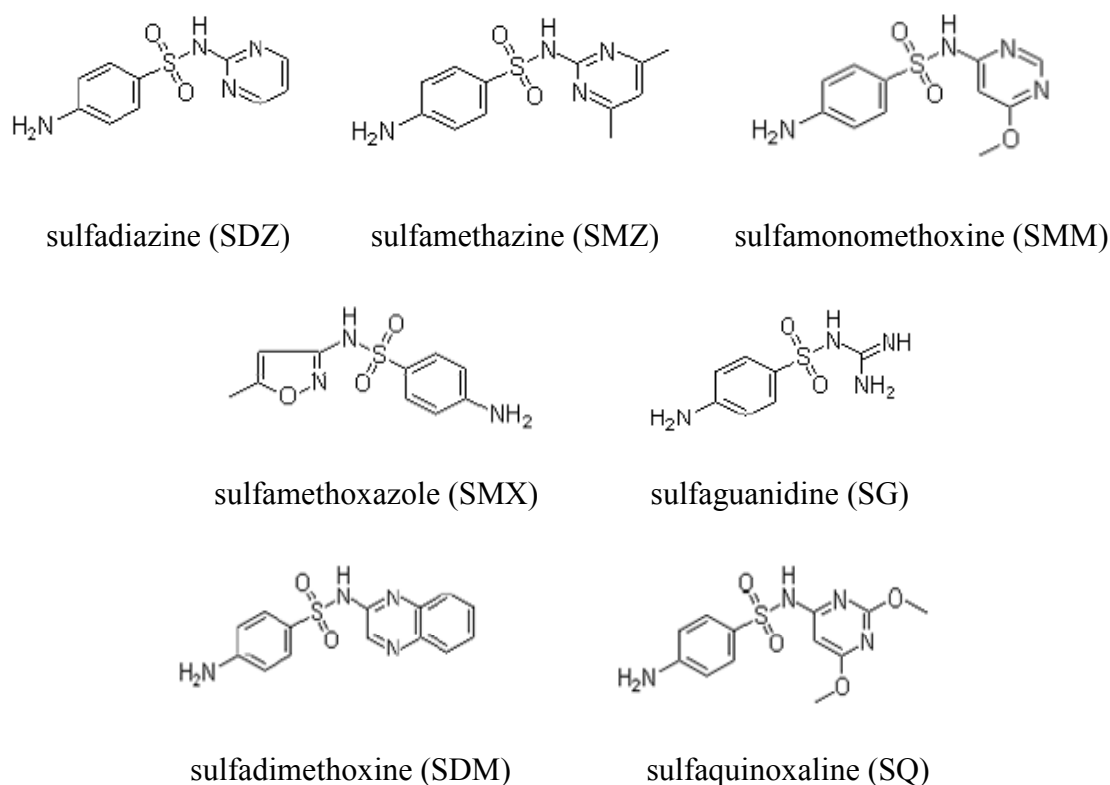


Figure 1.1 Chemical structures of the studied sulfonamides.

1.2 Research Objectives

Sequential-injection on-line solid-phase extraction coupled with HPLC-EC was developed for the separation and determination of sulfonamides (SAs). The developed method was then applied to the determination of sulfonamides in real samples.

1.3 Scope of Research

The sequential-injection system for on-line solid-phase extraction coupled with HPLC-EC was utilized for the determination of seven SAs. The effects of eluent, sample loading and eluting rate, eluate zone, linearity, limit of detection, and limit of quantitation on the separation and determination of SAs were studied in detail.

CHAPTER II

THEORY

2.1 Flow-Analysis Techniques

Flow-based methods are well established and widely used as automated methods for analysis. In this section two flow-based methods, flow injection analysis and sequential injection analysis, are discussed.

2.1.1 Flow Injection Analysis [34]

Flow injection analysis (FIA) is a well-established continuous-flow technique that has proven its utility in both basic research and practical applications. This technique was initiated almost simultaneously in the mid 1970s by Ruzicka and Hansen [35] in Denmark and Stewart and coworkers [36] in the United States. The principle of this technique was to exploit controlled dispersion in narrow bore tubing, sometimes called “zone fluidics”. A typical FIA manifold is illustrated in Figure 2.1. To carry out the technique, a volume of sample is inserted into the sample loop of an injection valve while a stream of carrier and a stream of reagent are mixed at a confluence point, flowing constantly through the detector. After the sample loop is filled with the sample, the valve is rotated so that the sample is injected into the flowing carrier stream and physically transported by the carrier to the confluence point, where it mixes with the reagent. In the course of its travels through the reaction coil, the sample zone disperses and reacts with the reagent to form a detectable species. The detectable species gives rise to a transient peak when it passes through the flow-cell of the detector.

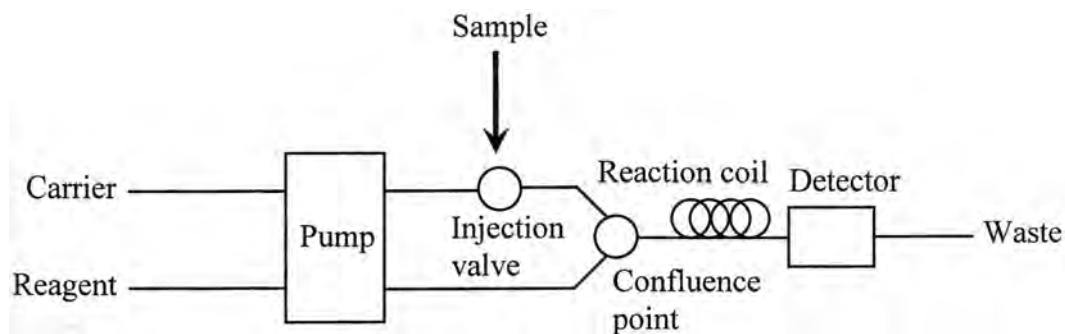


Figure 2.1 A typical manifold for flow injection analysis.

2.1.2 Sequential Injection Analysis [34,37,38]

Sequential injection analysis (SIA) was first proposed by Ruzicka and Marshall [39] in 1990 as a possible alternative to FIA. The principles upon which SIA is based are similar to those of FIA, namely controlled partial dispersion and reproducible sample handling. In contrast to FIA, SIA employs a computer-controlled multi-position selection valve and bi-directional pump operated synchronously. A typical SIA manifold is illustrated in Figure 2.2.

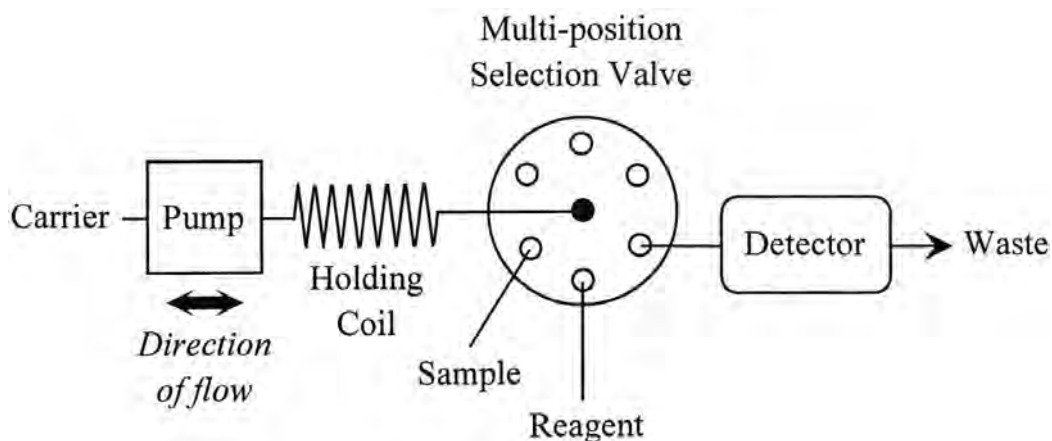


Figure 2.2 A typical manifold for sequential injection analysis.

Propulsion of solution through the manifold tubing (typically 0.5-0.8 mm i.d., PTFE) is achieved using a peristaltic pump or a syringe pump. A holding coil is placed between the pump and the common port of the multi-position selection valve. The selection ports of the valve are coupled to sample and reagent reservoirs as well

as the detector. The valve is directed to a selection port that is connected to the sample line and a zone of the sample is drawn up into the holding coil by the pump. Then, the selection valve is directed to a port that is connected to a reagent line and a zone of the reagent is drawn up into the holding coil adjacent to the sample zone. Next, the selection valve is switched to a port that is connected to a detector. As the zone moves towards the detector, zone dispersion and overlap occur, resulting in the formation of the detectable species that is monitored by the detector. The vast majority of SIA procedures are still based on the solution-phase chemistry described above.

Comparing SIA and FIA for simple sample manipulation, the following points were made in Table 2.1.

Table 2.1 Comparison between SIA and FIA.

SIA	FIA
A simpler, more robust single channel manifold even with multi-component chemical systems.	Simplicity and low cost instrumentation
Syringe pumps offer increased robustness with precise operation and little maintenance for process applications.	Multi-channel peristaltic pumps
Sample and reagent consumptions are minimized due to the discontinuous operation mode.	High sampling rate
Selection valve provides a means for performing convenient automated calibration.	Reduced analyses cost when a lot of samples have to be analyzed
Accurate handling of sample and reagent zones necessitates computer control, so automation becomes essential.	Automation in sample preparation and detection

In recent years, it has become apparent that the scope of SIA can be extended to encompass a wide variety of more complex, on-line, sample-manipulation and pretreatment procedures. In these systems, the ports of the multi-position selection valve are coupled to various units (e.g., reservoirs, detectors, pumps, reactors, separators, special cells, and other manifolds), as illustrated in Figure 2.3 [40]. After aspiration of the sample zone into the holding coil via the sample line, the sample can be manipulated in different ways within the SIA manifold by taking advantage of the stopped-flow, bi-directional nature of fluid handling in SIA.

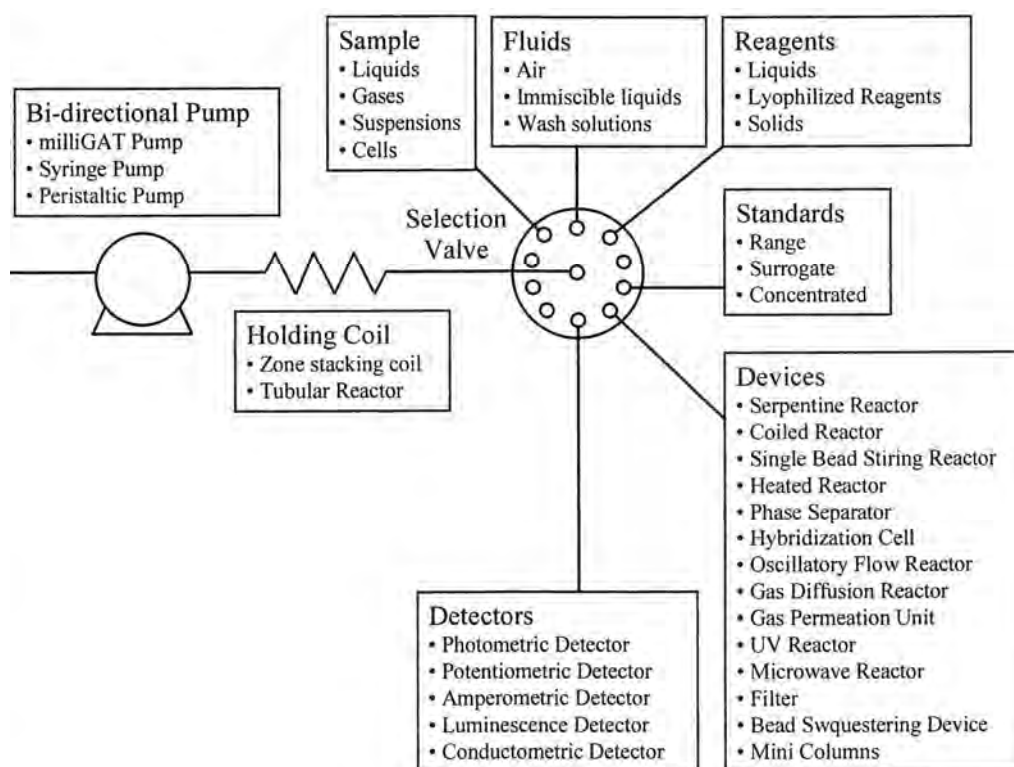


Figure 2.3 Different potential uses of SIA in automated sample pre-treatment.

2.2 High Performance Liquid Chromatography (HPLC) [41, 42]

High performance liquid chromatography is widely used for the separation of two or more compounds in a mixture by distributing them between two phases: (a) a stationary phase, which can be a solid or liquid supported on a solid; and (b) a mobile phase, which is liquid and flows continuously over the stationary phase. The separation of individual components results primarily from difference in their affinity

for the stationary phase. Figure 2.4 shows the four most widely used types of HPLC instruments. These methods include: (1) partition or liquid-liquid chromatography; (2) adsorption or liquid-solid chromatography; (3) ion exchange chromatography; and (4) size exclusion chromatography, including gel permeation chromatography and gel filtration chromatography. The schematics for the four modes of liquid chromatography are diagrammed in Figure 2.5. This research presented here will focus specifically on adsorption chromatography.

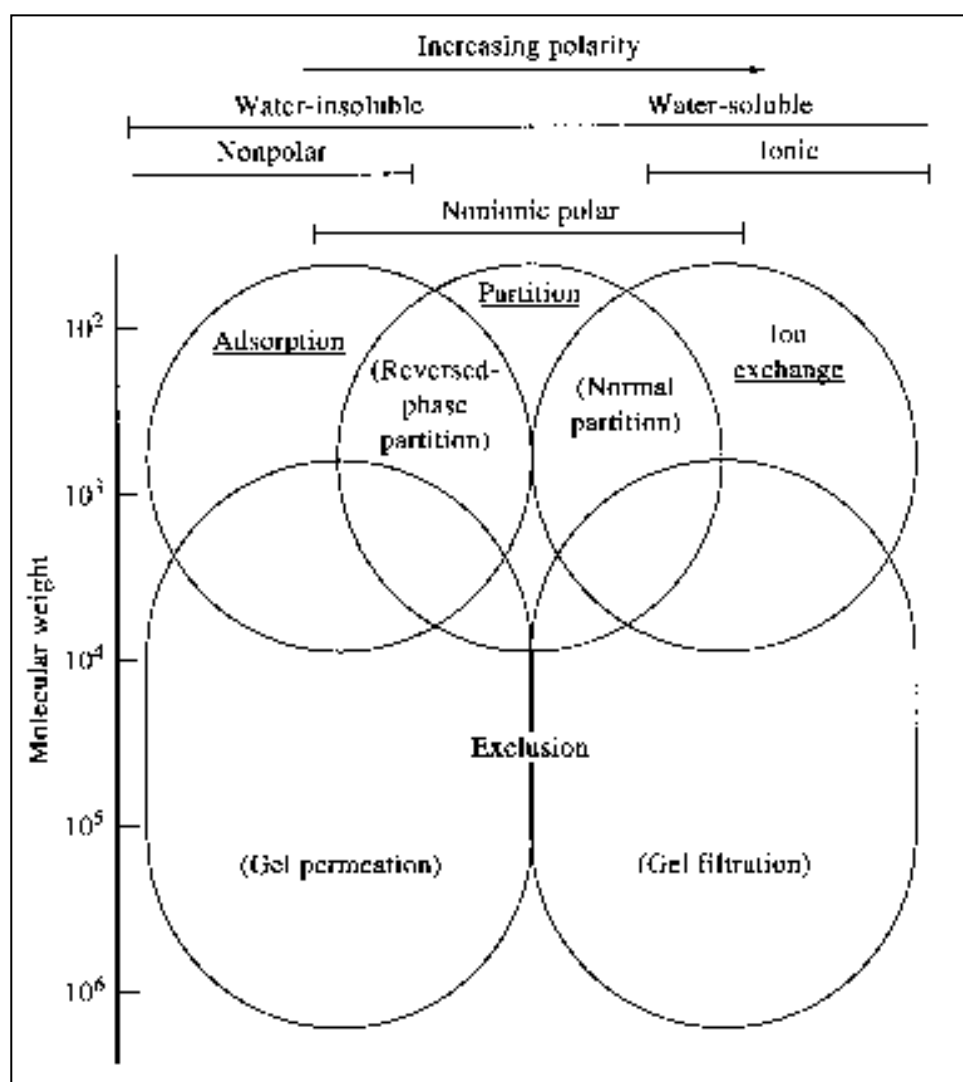
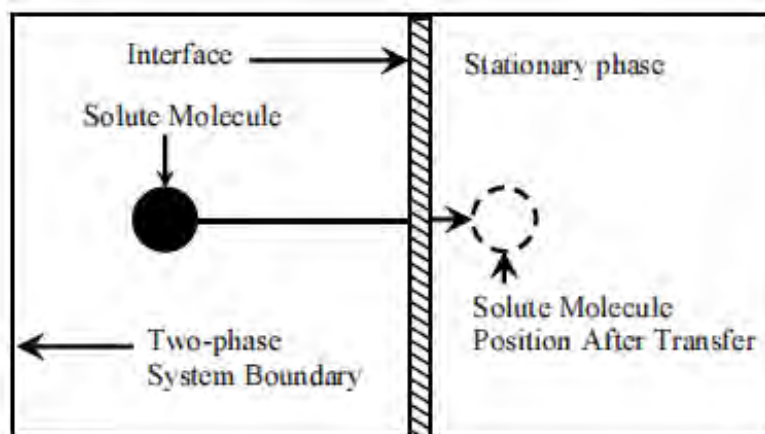
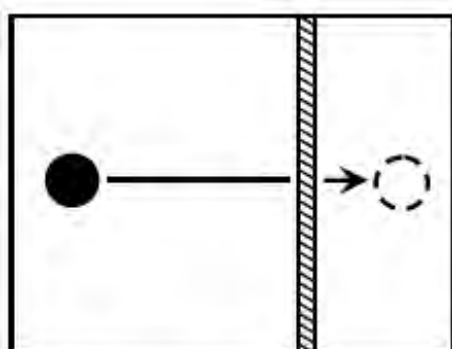


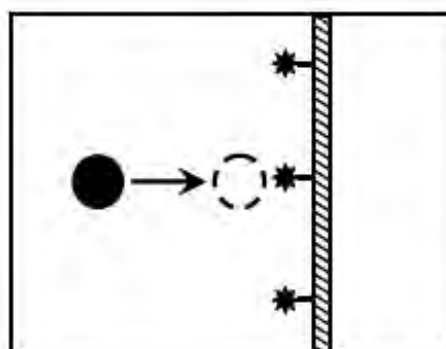
Figure 2.4 Types of liquid chromatography.



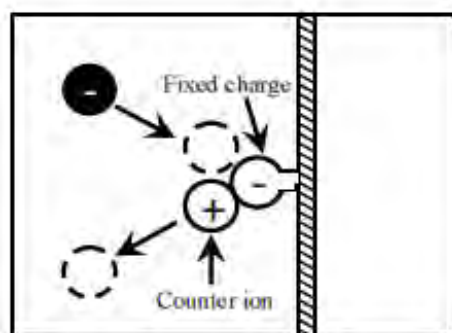
A. Transfer of solute to a Generalized Stationary Phase



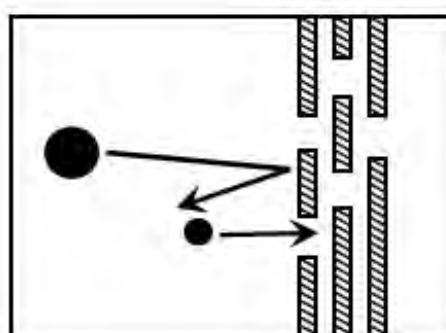
B. Liquid-Liquid



C. Liquid-Solid



D. Ion-Exchange



E. Exclusion

Figure 2.5 Schematic representations of the four modes of liquid chromatography.

2.2.1 High Performance Adsorption Chromatography [43]

Adsorption chromatography (Figure 2.5 (C)), often referred to as liquid-solid chromatography, is based on interactions between the solute and fixed active sites on a solid adsorbent used as the stationary phase. The adsorbent can either be packed in a column or spread on a plate. This adsorbent is generally an active, porous solid with a large surface area, such as silica gel, alumina or charcoal. The active sites, such as silanol groups on silica gel, typically interact with the polar functional groups of the compounds to be separated. The nonpolar portion of the molecule, however, has only a very minor influence on the separation.

2.2.2 Instrumentation [41,44]

HPLC is frequently used in biochemistry and analytical chemistry to separate, identify, and quantify compounds. HPLC utilizes a column that holds chromatographic packing material (stationary phase), a pump that moves the mobile phase through the column, and a detector that determines the retention times of the molecules. The variation in retention times depend on the interactions between the target analyte, the stationary phase, and the solvent used. Figure 2.6 depicts a diagram of the important components for a typical HPLC instrument.

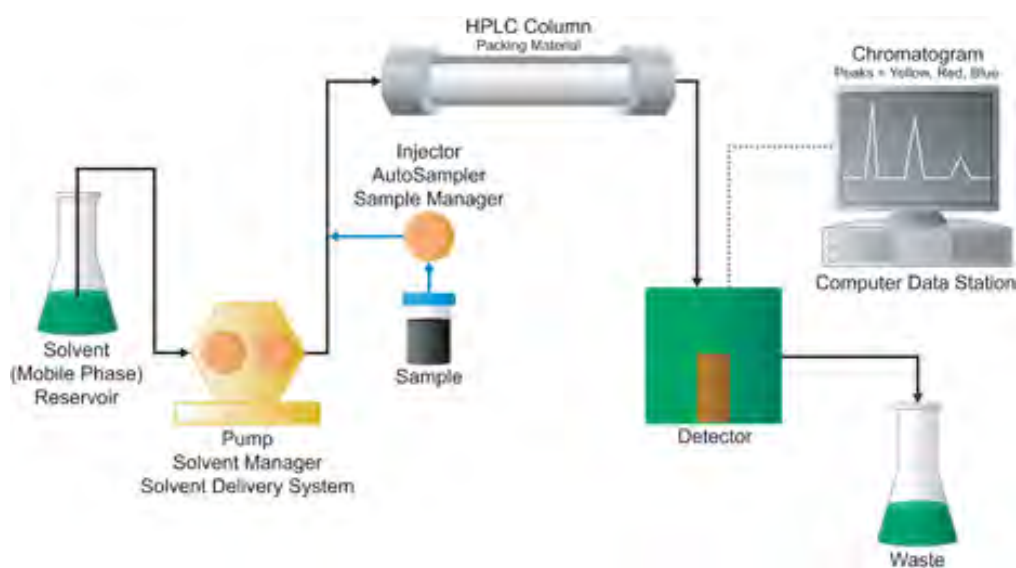


Figure 2.6 Important components of a typical HPLC instrument.

2.2.2.1 Mobile Phase Reservoir

The reservoirs are storage containers made of material resistant to chemical attack by the mobile phase. In most common systems, the reservoirs are either 1 or 2 liter glass bottles. It is often necessary, and usually preferable, to remove dissolved air from the mobile phase before it is fed to the pump, a procedure called mobile phase degassing. Degassing can be achieved by helium dispersion, applying vacuum to the mobile phase, ultrasonication, or heating. Bubbles of dissolved gases can cause the operation of the HPLC pump to become unreliable, leading to fluctuations in flow rate. Bubbles can also get trapped in the detector flow cell, causing problems with this module as well.

The mobile phase is typically comprised of a single solvent or a solvent mixture. Use of a constant composition is referred to as isocratic elution, while gradient elution is the sequential use of two (and sometimes more) solvent systems that significantly differ in polarity. The ratio of the two solvents is varied in a preprogrammed way during the separation, sometimes continuously and sometimes in a series of steps.

2.2.2.2 Pump

The requirements for liquid chromatographic pumps include: (1) ability to generate pressures of up to 6,000 psi, (2) pulse-free output, (3) flow rates ranging from 0.1 to 10 mL min⁻¹, (4) a flow reproducibility of 0.5 % or better, and (5) resistance to corrosion by solvents. The types of pumps used in liquid chromatography can be divided into two categories according to the mobile phase dispensing mechanism: constant volume pumps (e.g., reciprocating pumps and syringe pumps) or constant pressure pumps (e.g., pneumatic pumps).

Syringe pumps dispense liquid using solvent displacement by a mechanically controlled piston advancing at a constant rate in a fixed-volume chamber (250-500 mL capacity). The pump output is relatively pulse-free, of very high pressure, and gradient and flow programming are quite straightforward. The disadvantages of this

type of pump are high cost, limited solvent reservoir capacity, and problems with solvent compressibility.

The reciprocating type of pump is the most widely used in HPLC systems. This device consists of a small cylindrical chamber that is filled and then emptied by the back-and-forth motion of a piston. The pumping motion produces a strong, pulsed flow that must be subsequently damped. Advantages of the reciprocating pump include small internal volume, high output pressure (up to 10,000 psi), readily adaptable to gradient elution, and constant flow rates, which are largely independent of column backpressure and solvent viscosity. Because of these reasons, most modern commercial chromatographs employ a reciprocating pump. Yet other some instruments use a pneumatic pump, which consists of a solvent container housed in a vessel that can be pressurized by compressed gas. This type of pump is inexpensive and pulse-free. The limits on solvent capacity and pressure output are major disadvantages and pumping rate depends on solvent viscosity. Furthermore, these pumps cannot be adapted to gradient elution.

2.2.2.3 Injector

The most commonly used sample injector in HPLC is the loop injector. A six-port, high pressure, external loop injector and its basic operating principles are illustrated in Figure 2.7. In the load position, sample is forced through the loop by a syringe. Once the loop is completely filled, the valve core is rotated either manually or by an automatic air-operated or electrically-operated actuator. The chromatographic pump then forces mobile phase through the loop and displaces the load to the column. To refill the loop, the core is rotated back to the load position.

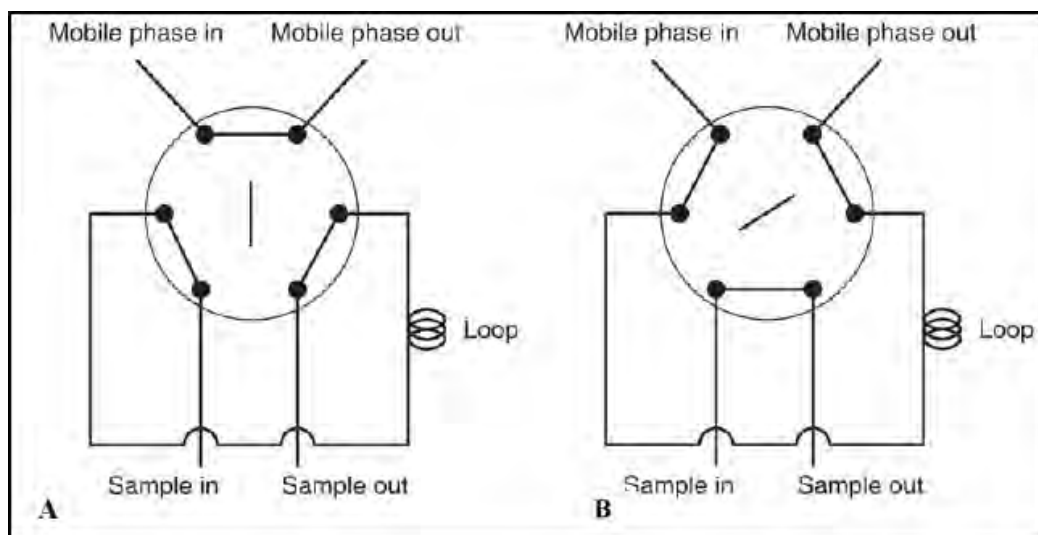


Figure 2.7 Schematic diagram of a loop injector in the (A) load and (B) inject positions.

2.2.2.4 Columns

Typically, there are two types of columns in an HPLC system: an analytical column and a guard column. The guard column is placed before the analytical column to protect it from contamination. Guard columns usually contain the same particulate packing material as the analytical column, but they are significantly shorter and less expensive. For analytical columns, the conventional columns used are particle-packed columns. The most widely used type of particle-packed column has bonded-phase packing. Bonded-phase packing is where a liquid film is coated on a packing material consisting of 3-10 μm porous silica particles. The stationary phase may be partially soluble in the mobile phase, causing it to “bleed” from the column over time. To prevent loss of the stationary phase, it is covalently bound to the silica particles. Bonded stationary phases are attached by reacting the silica particles with an organochlorosilane of the general form $\text{Si}(\text{CH}_3)_2\text{RCl}$, where R is an alkyl or substituted alkyl group.

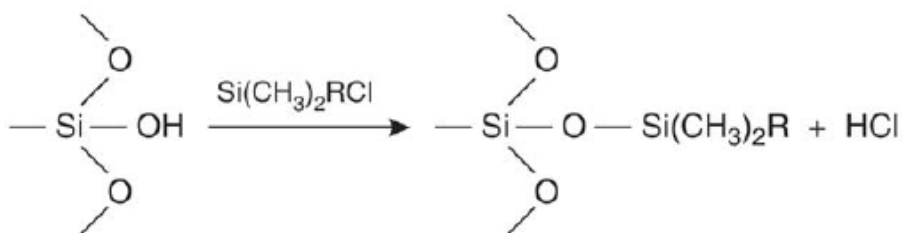


Figure 2.8 Reaction of bonded stationary phase with organochlorosilanes.

The disadvantages of particle-packed columns are high flow resistance, high backpressure and particle splitting at elevated flow rates. These drawbacks can lead to non-reproducibility, low separation efficiency and reduced sample throughput.

Recently, monolithic columns were discovered and verified as an alternative material to conventional columns. Monolithic columns are classified according to their base, such as a polymer- or silica-based monolithic column. The polymer-based monolithic column is prepared by polymerization of a monomer. The excellent properties of the polymer-based monolithic columns are suitable for large molecule separation and can be used over a wider pH range than the silica-based monolithic columns. However, these polymer-based columns are easily swollen or shrunk in organic solvent. Silica-based monolithic columns are prepared by a sol-gel process and are used for the separation of small- or medium-sized molecules. The advantage of this column over the polymer-based monolithic column is that it provides a high tolerance to organic solvent, which leads to a longer column lifetime. The research presented here will focus on the use of silica-based monolithic columns.

2.2.2.5 Silica-Based Monolithic Columns

2.2.2.5.1 Formation Processes and Pore Structure Control of Silica Monoliths

The starting silica sources for silica-based monolithic columns are tetramethoxysilane, tetraethoxysilane or *n*-alkyltrialkoxysilanes, which are subjected to acid catalyzed hydrolysis and condensation in the presence of water-soluble polymers, such as polyethyleneglycols and polyacrylic acid with surfactants as

additives. The multicomponent solution converts into a sol-gel system through a nucleation and growth mechanism in which small fractions of a finely dispersed phase grow in size (see Figure 2.9 (A)) that is limited by a thermally-activated diffusion process. A second process, called spinodal decomposition, also takes place, leading to a co-continuous domain structure, which remains stable over an extended period of time (see Figure 2.9 (B)). Gel morphology is controlled by the kinetics of two competitive processes: domain coarsening and structure freezing in the sol-gel transition. The resulting gels are aged and a solvent exchange is performed to tailor the pore structure. The macroporous gel domains, which have been burned out by calcination, are filled with the polymer. The mesopore structure and mesopore size are adjusted by hydrothermal treatment conditions. In this way, the process enables the generation of two continuous pore systems where adjustment and control of pore size and the porosity of macropores and mesopores, independently. The manufacturing process of monolithic silica rods with 4.6 mm I.D. is done by first comprising the following consecutive step: preparing the starting sol, then carrying out phase separation and gelation, and finishing with aging and drying. After drying, the rods are clad with poly(ether-ether ketone) (PEEK). Further surface functionalization is then performed *in situ*. The product is called Chromolith Performance and marketed by Merck (Darmstadt, Germany).

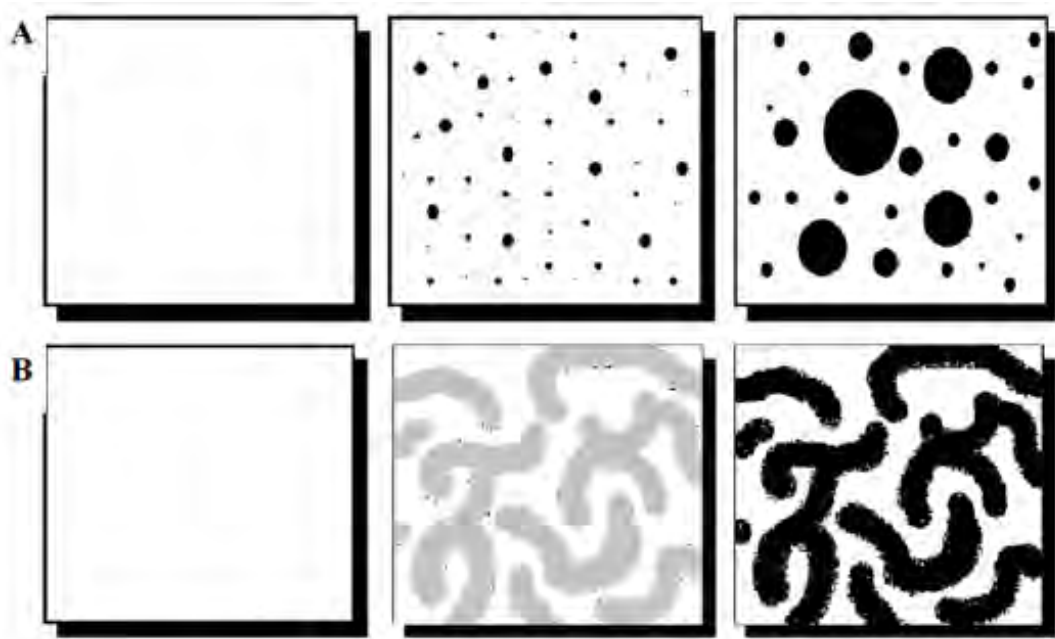


Figure 2.9 (A) Nucleation and growth (diffusion limited) of silica-based monoliths (B) Spinodal decomposition (spontaneous) of silica-based monoliths.

The bimodal pore structure of a Chromolith column is characterized by a distinct bimodal pore structure where macropores of 2 μm in diameter and mesopores with an average pore diameter of approximately 13 nm coexist in the same column material. The total porosity of the monolithic columns amount to 80% or higher, with the larger proportion accounted for by macropores. The mesopores generate a specific surface area of approximately $300 \text{ m}^2\text{g}^{-1}$ in the column material. Silica monoliths (rod) of 4.6 mm. I.D. size were characterized by classical pore structure analyses, such as nitrogen sorption at 77 K, mercury intrusion, scanning electron microscopy (SEM) and transmission electron microscopy (TEM). SEM photographs for the bimodal pore structure of silica-based monolithic columns are illustrated in Figure 2.10. Using these methods, the mesopore and macropore volume distributions were assessed to determine the size of the diffusive and flow-through pores.

Monolithic columns have characteristic single piece, through-pore, high porosity, or cross-linked skeletons. The advantages of monolithic columns are lower back-pressures, even at high flow rates, and separations that can be performed in a shorter analysis time and higher sample throughput than particle-packed columns.

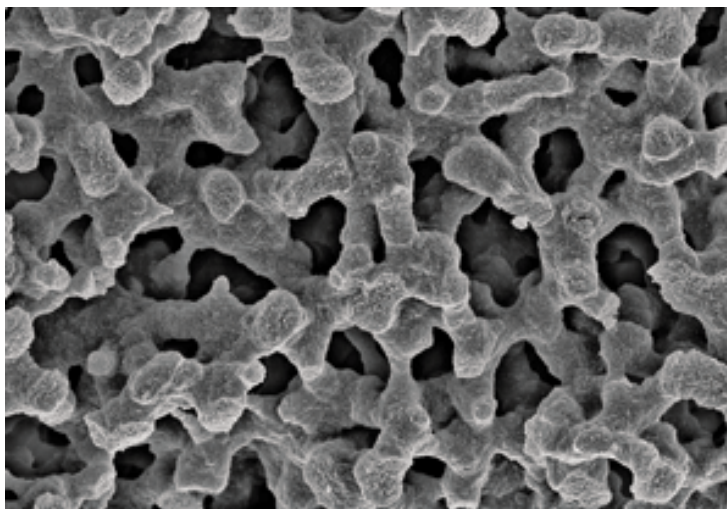


Figure 2.10 SEM photographs for the bimodal pore structure of silica-based monolithic columns.

2.2.2.6 Detectors

The detector measures the signal corresponding to the concentration of sample bands as they move off the analytical column and pass through the detector flow cell. An ideal detector of any type is sensitive to low concentrations of analyte, provides linear response, and does not broaden the eluted peaks. The detector should also be insensitive to changes in temperature and solvent composition. Additionally, to prevent peak broadening, the detector volume should be less than 20% of the volume of the chromatographic band. Gas bubbles in the detector create noise, so the mobile phase must be degassed beforehand. The common types of detectors used are absorbance, fluorescence, refractive index, mass spectrometry, FTIR, light scattering, optical activity, element selective, and photoionization. The most popular detectors among those listed are spectroscopic detectors and electrochemical detectors.

Spectroscopic detectors, the most popular HPLC detectors, are based on spectroscopic measurements, including UV/Vis absorption, and fluorescence.

Electrochemical detectors, another common group of HPLC detectors, are those based on electrochemical measurements such as voltammetry, amperometry, conductivity, and coulometry.

2.3 Fundamentals of Electrochemistry

Electrochemistry encompasses chemical and physical processes that involve the transfer of charge. There are two categories of electrochemical processes, potentiometric and electrolytic, that are applied to quantitative measurements. Potentiometry is the field of electroanalytical chemistry (EC) in which potential is measured under the conditions of no current flow. The measured potential may then be used to determine the analytical quantity of interest, generally the concentration of some component of the analyte solution. Unlike potentiometry, where the free energy contained within the system generates the analytical signal, electrolytic methods are an area of electroanalytical chemistry in which an external source of energy is supplied to drive an electroanalytical reaction that would not normally occur. This externally applied driving force is either an applied potential or current. When potential is applied, the resultant current is the analytical signal; and when current is applied, the resultant potential is the analytical signal. Techniques that utilize applied potential are typically referred to as voltammetric methods, while those with applied current are referred to as galvanostatic methods. Unlike potentiometric measurements, which employ only two electrodes, voltammetric measurements utilize a three electrode electrochemical cell. The use of three-electrodes (working, auxiliary, and reference), along with the potentiostat instrument, allows accurate application of potential functions and the measurement of the resultant current. The different voltammetric techniques are distinguished from each other primarily by the potential function that is applied to the working electrode to drive the reaction and by the material used as the working electrode. In this section, some voltammetric techniques used in this work, such as cyclic voltammetry and amperometric detection, are considered.

2.3.1 Mass transport [41]

Reactants or charges are transported to the surface of an electrode by three mechanisms: (1) diffusion, (2) migration, and (3) convection. Products are removed from electrode surfaces in the same way.

2.3.1.1 Diffusion

When there is a concentration difference between two regions of the solution, ions or molecules move from the more concentrated region to the more dilute. This process is called diffusion and ultimately leads to a disappearance of the concentration gradient. The rate of diffusion is directly proportional to the concentration difference.

2.3.1.2 Migration

The electrostatic process by which ions move under the influence of an electric field is called migration. The rate at which ions migrate to or away from an electrode surface generally increases as the electrode potential increases. This charge movement constitutes a current, which also increases with potential. Migration causes anions to be attracted to the positive electrode and cations to the negative electrode. Migration of analyte species can be minimized by having a high concentration of an inert electrolyte, called a supporting electrolyte, present in the cell. The current in the cell is then primarily due to charges carried by ions from the supporting electrolyte.

2.3.1.3 Convection

Reactants can also be transferred to or from an electrode by mechanical means. Forced convection, such as stirring or agitation, tends to decrease the thickness of the diffusion layer at the surface of an electrode and thus decrease concentration polarization.

2.3.2 Voltammetry [43,45-47]

Voltammetry experiments investigate the half-cell reactivity of an analyte. Most experiments control the potential of an electrode in contact with the analyte while measuring the resulting current, and to conduct such an experiment requires at least two electrodes. The working electrode, which makes contact with the analyte, must apply the desired potential in a controlled way and facilitate the transfer of electrons to and from the analyte. A second electrode acts as the other half of the cell. This second electrode must have a known potential with which to gauge the potential of the working electrode, and it must also balance the electrons added or removed by the working electrode. While this is a viable setup, it has a number of shortcomings. Most significantly, it is extremely difficult for an electrode to maintain a constant potential while passing current to counter redox events at the working electrode.

To solve this problem, the role of supplying electrons and referencing potential has been divided between two separate electrodes. The reference electrode is a half-cell with a known reduction potential. Its only role is to act as reference in measuring and controlling the working electrodes potential and at no point does it pass any current. The auxiliary electrode passes all the current needed to balance the current observed at the working electrode. To achieve this current, the auxiliary will often swing to potentials at the edges of the solvent window, where it oxidizes or reduces the solvent or supporting electrolyte. These electrodes, the working, reference, and auxiliary, make up the modern three-electrode system. There are many systems that have more electrodes, but their design principles are generally the same as the three-electrode system. For example, the rotating ring-disk electrode has two distinct and separate working electrodes, a disk and a ring, which can be used to scan or hold potentials independently of each other. Both of these electrodes are balanced by a single reference and auxiliary combination for a total of four electrodes. More complicated experiments may add working electrodes or reference and auxiliary electrodes as needed.

In practice it can be very important to have a working electrode with known dimensions and surface characteristics. As a result, it is common to clean and polish working electrodes regularly. The auxiliary electrode can be almost anything as long

as it doesn't react with the bulk of the analyte solution and conducts well. The reference is the most complex of the three electrodes with, a variety of different standard materials used worth investigating elsewhere. For non-aqueous work, IUPAC recommends the use of the ferrocene/ferrocenium couple as an internal standard. In most voltammetry experiments, a bulk electrolyte (also known as the supporting electrolyte) is used to minimize solution resistance. It can be possible to run an experiment without a bulk electrolyte, but the added resistance greatly reduces the accuracy of the results. In the case of room temperature ionic liquids, the solvent can act as the electrolyte. The waveforms of the three most common excitation signals used in voltammetry are shown in Figure 2.11. The classical voltammetric excitation signal is a linear scan, as shown in Figure 2.11(a). The potential applied to a cell of this excitation increases linearly as a function of time. The two-pulse excitation signals are shown in Figure 2.11(b) and Figure 2.11(c). The current responses of the pulse type are measured at various times during the lifetime of these pulses.

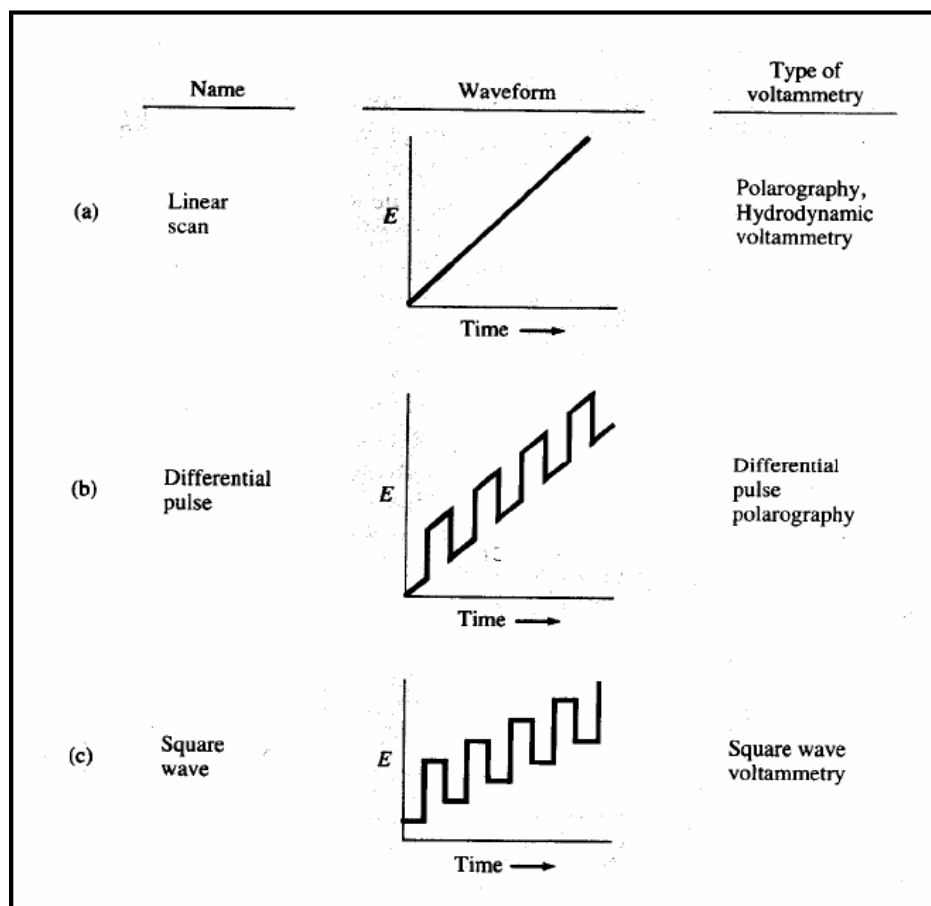


Figure 2.11 Typical excitation signals for voltammetry.

2.3.3 Cyclic Voltammetry [48-51]

Cyclic voltammetry (CV) is a very useful electrochemical technique in many areas of chemistry. It is rarely used for quantitative determinations, but it is widely used for studying the mechanisms and reversibility of electrode processes. This technique is based on varying the applied potential at a working electrode in both the forward and reverse directions while monitoring the current. In CV, the triangular waveform shown in Figure 2.12 is applied to the working electrode. After the application of a linear voltage ramp between times t_0 and t_1 (typically a few seconds), the ramp is reversed to bring the potential back to its initial value at time t_2 . This cycle may be repeated many times. The initial portion of the cyclic voltammogram in Figure 2.13, beginning at zero, exhibits a cathodic wave. Instead of leveling off at the top of the wave, current decreases at more negative potentials because the analyte becomes depleted near the electrode, as diffusion is too slow to replenish analyte near

the electrode. At the time of peak voltage, the cathodic current has decayed to a small value, as can be seen in Figure 2.13. Afterwards, the potential is reversed and, eventually, reduced product near the electrode is oxidized, thereby giving rise to an anodic wave. Finally, as the reduced product is depleted, the anodic current decays back to its initial value.

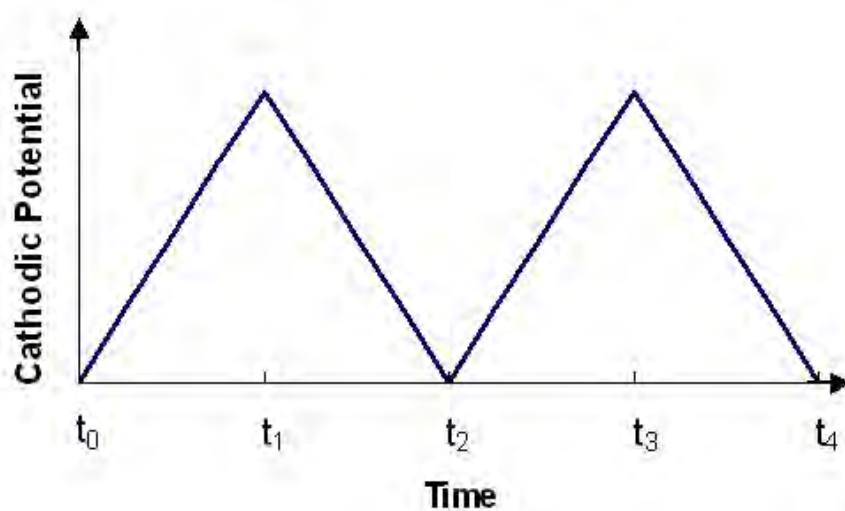


Figure 2.12 Cyclic voltammetry waveform.

Figure 2.13 illustrates a reversible reaction that is fast enough to maintain the equilibrium concentrations of reactant and product at the electrode surface. The anodic peak and cathodic peak currents have equal magnitudes in a reversible process, and

$$E_{pa} - E_{pc} = \frac{2.303RT}{nF} = \frac{60.0 \text{ (mV)}}{n} \text{ (at } 25^{\circ}\text{C)} \quad \text{(equation 2.1)}$$

where E_{pa} and E_{pc} are the potentials at which the anodic peak and cathodic peak currents are observed, and n is the number of electrons in the half-reaction. The half-wave potential, $E_{1/2}$, lies midway between the two peak potentials. The formal reduction potential (E^0) in a reversible reaction is given by

$$E^0 = \frac{E_{pc} + E_{pa}}{2} \quad \text{(equation 2.2)}$$

For an irreversible reaction, the cathodic and anodic peaks are drawn out and more separated. At the limit of irreversibility, where the oxidation is very slow, no anodic peak is seen.

For a reversible reaction, the peak current (I_p , amperes) for the forward sweep of the first cycle is proportional to the concentration of analyte and the square root of the sweep rate:

$$I_p = (2.686 \times 10^5) n^{3/2} A C D^{1/2} v^{1/2} \quad (\text{at } 25^\circ\text{C}) \quad (\text{equation 2.3})$$

where n is the number of electrons in the half-reaction, A is the area of the electrode (cm^2), C is the concentration (mol/cm^3), D is the diffusion coefficient of the electroactive species (cm^2/s), and v is the sweep rate (V/s). The faster the sweep rate, the greater the peak current as long as the reaction remains reversible. If the electroactive species is adsorbed on the electrode, the peak current is proportion to v rather than \sqrt{v} .

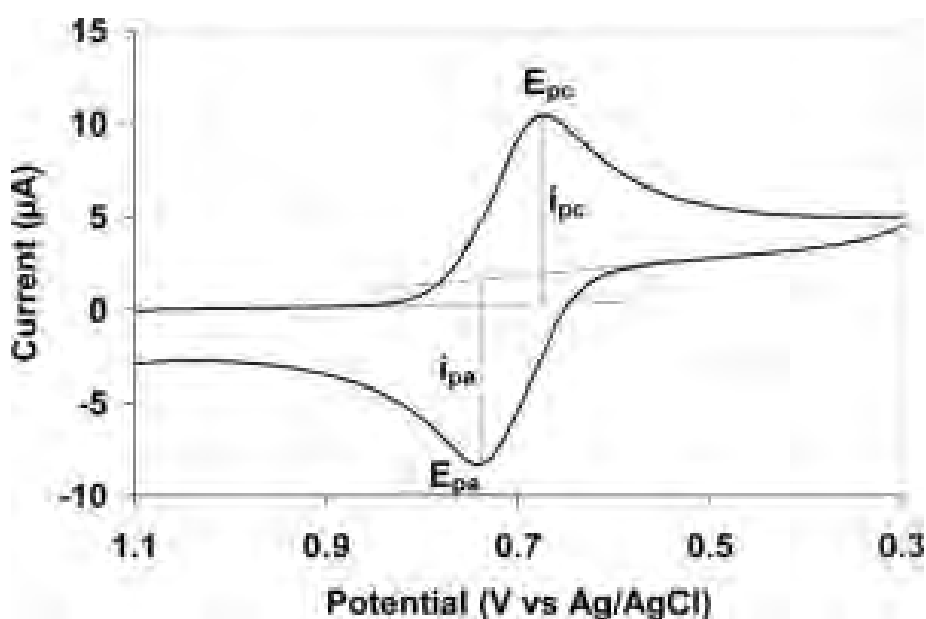


Figure 2.13 Typical cyclic voltammogram where i_{pc} and i_{pa} show the peak cathodic and anodic currents (respectively) for a reversible reaction.

2.3.4 Amperometry [52-53]

Amperometric detection has been developed as a sensitive method for chromatographic detection of electroactive solutes or as a detection method in conjunction with a selective biocatalytic step in biosensors. It has also been used as a detection method in flow analysis techniques. Amperometric detection is based on oxidation or reduction of an electrochemically active analyte at a working electrode held at a potential that is high enough to initiate the oxidation or reduction process. The electric current resulting from this electrochemical reaction serves as the analytical signal and is directly proportional to the concentration of analyte. Generally, the flow conditions in measurements with amperometric detection decrease the thickness of the diffusion boundary layer at the working electrode surface. This results in an increase in the measured current.

The potential applied to the working electrode may be constant or it may be applied in a pulsed mode. Typical potential waveforms used in amperometric detection are illustrated in Figure 2.14.

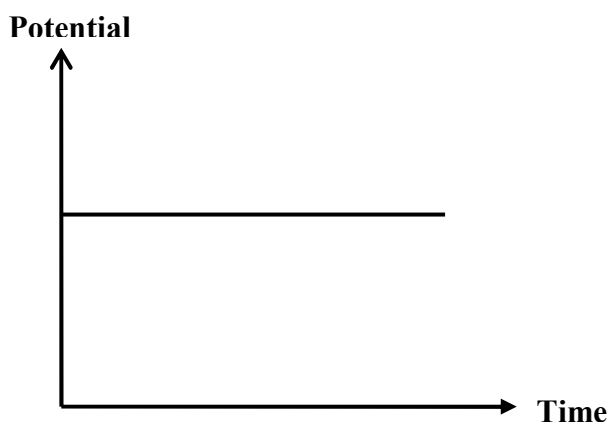


Figure 2.14 A typical waveform in amperometry.

2.3.5 Working electrode

The performance of the voltammetric procedure is strongly influenced by the material of the working electrode. The working electrode should provide high signal-to-noise ratios, as well as reproducible responses. Thus, its selection depends primarily on the redox behavior of the target analyte and the background current over the potential region required for the measurement. Other considerations include the potential, electrical conductivity, surface reproducibility, mechanical properties, cost, availability, and toxicity of the material. A range of materials has been applied as working electrodes for electroanalysis. The most popular materials are those involving mercury, carbon, and noble metals. This research will focus primarily on electrodes constructed from carbon.

Carbon exists in various conductive forms and its electron transfer kinetics depend on structure and surface preparation. Electrochemical reactions at carbon are normally slower than those of metallic electrode. Carbon is the most commonly used electrode material in electroanalytical chemistry and it is available in a variety of microstructures, including graphite, glassy carbon, carbon fiber, nanotubes, amorphous powders, and diamond. All of these structures are sp^2 carbons, except the diamond electrode, which contains sp^3 carbons.

2.3.5.1 Boron-doped diamond (BDD) [54-58]

Electrically conducting diamond is a new type of carbon electrode material that is beginning to find widespread use in electroanalysis. The material possesses superior properties over other forms of carbon, including (i) low and stable background current over a wide potential range, (ii) wide working potential window in aqueous media, (iii) weak molecular adsorption, (iv) dimensional stability and high corrosion resistance, (v) optical transparency, and (vi) relatively rapid electron transfer kinetics for several redox systems without conventional pretreatment. The material is now available from several commercial sources and is not overly expensive, as commonly perceived. Figure 2.15 is a comparison of the cyclic voltammetric current versus potential curves for boron-doped diamond thin film, glassy carbon, and Hg electrodes in 0.1 M H_2SO_4 .

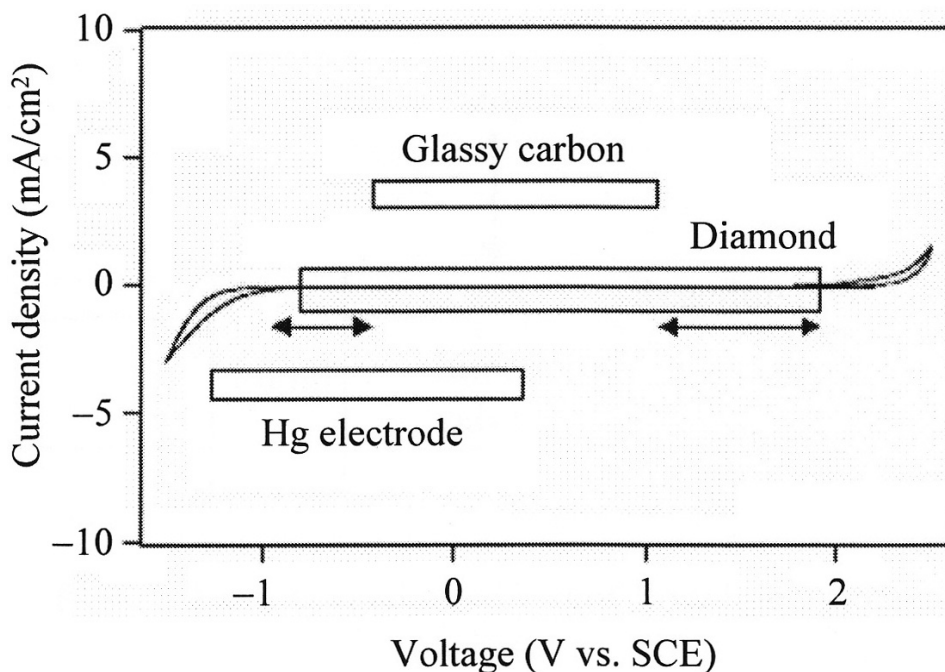


Figure 2.15 Cyclic voltammogram for diamond in 0.1 M H_2SO_4 . The range of potential windows for glassy carbon and Hg electrodes is shown for comparison.

Boron is by far the most widely used dopant to produce conducting diamond electrodes. This is because boron has a low charge carrier activation energy of 0.37 eV and boron doping leads to a p-type semiconductor. At low doping levels, the diamond acts as an extrinsic semiconductor, while at high doping levels, the material acts as a semimetal. To introduce boron into the diamond material during film growth, the boron-containing substance has to be added to the deposition gas mixture. Compounds such as diborane or trimethyl borane can be used for this purpose. The boron atoms substitute in place of some of the carbon atoms during film growth. Boron-doped diamond electrodes with resistivities between 5 and 100 $\text{m}\Omega\text{-cm}$ are usually produced from this process. Typical and useful boron concentrations in diamond are between 500 ppm and about 10,000 ppm, or $10^{19} - 10^{21}$ atoms cm^{-3} . An SEM image of boron-doped crystalline diamond is shown in Figure 2.16.

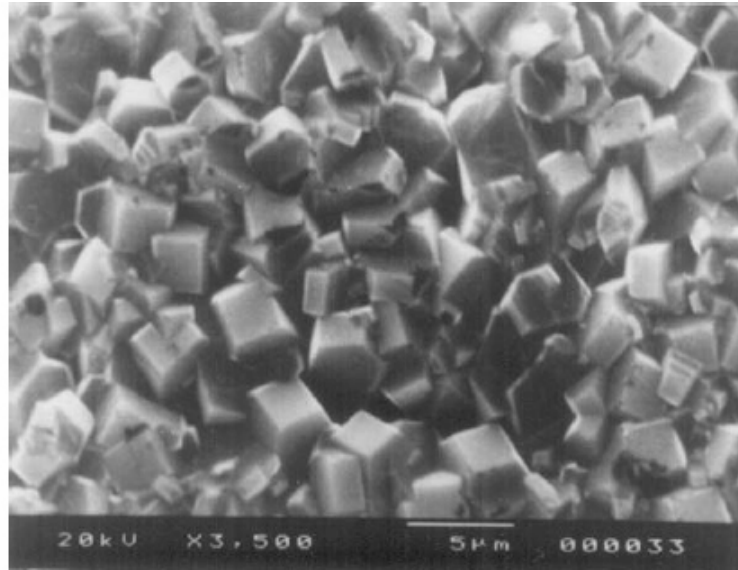


Figure 2.16 SEM image of a boron-doped crystalline diamond.

The most common method for CV other than using boron dopants is microwave plasma CVD because of the commercial availability of such reactor systems. While the mechanisms of film growth are somewhat different among each method, all of them serve to activate a carbonaceous source gas to produce a growth precursor in close proximity to the substrate surface. A typical CVD reactor consists of the growth chamber and equipment associated with the particular activation method (e.g., microwave power source), as well as various accessories, such as mass flow controllers for regulating the source gases, a throttle exhaust valve and controller for regulating the system pressure, a pumping system, temperature measurement capability, and a gas handling system for supplying the source gases. A block diagram of a typical CVD system is shown in Figure 2.17.

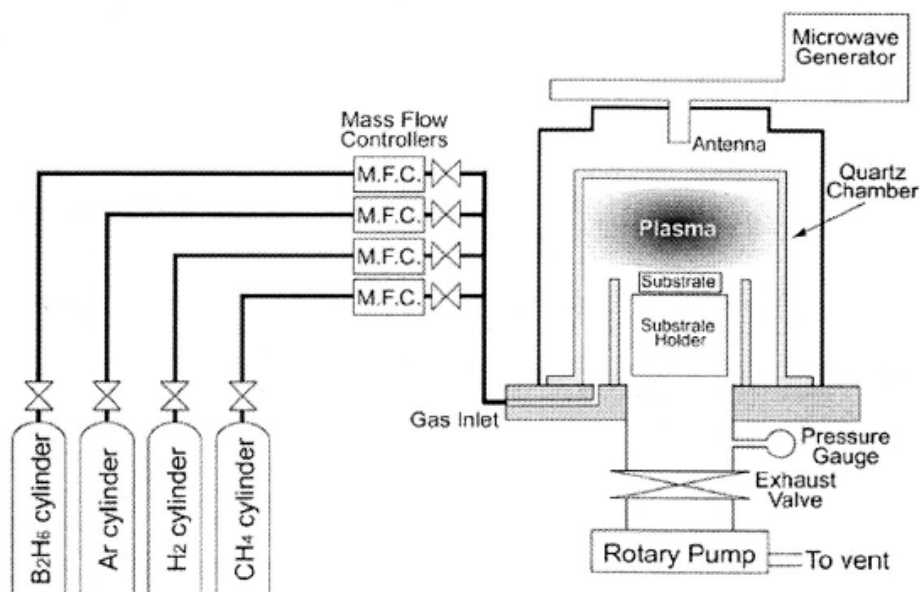


Figure 2.17 Block diagram of a typical microwave plasma CVD reactor.

In the case of microwave assisted CVD, the microwave energy from the generator is pointed to, and focused within, a quartz cavity to produce a spherically shaped, glow-discharge plasma directly above the substrate. The substrate can be positioned either outside of (a few mm), or immersed within the intense discharge region. The plasma is where the reactive species involved in the diamond growth are formed. The key deposition parameters are the source gas composition, microwave power, system pressure, and substrate temperature.

2.3.6 Flow Cell for Electrochemistry [59]

A typical thin-layer amperometric flow cell is shown in Figure 2.18. A gasket held between a stainless-steel block and a polymeric block defines the thin-layer channel. The stainless-steel block is the auxiliary electrode and provides a compartment for the reference electrode, while the polymeric block contains the working electrode. This design and, in fact, nearly all cell designs, incorporate working, auxiliary, and reference electrodes. The potential selected by the user is applied between the reference and working electrodes while the current is passed between the auxiliary and working electrodes. Detection occurs at the working electrode in the thin-layer region. Electrodes of the same or different materials may

be interchanged by simply swapping the working electrode half of the thin-layer cell. Carbon pastes, glassy carbon, mercury on gold, platinum, and silver have all been used for this purpose. This design allows easy collection of solute bands without appreciable dispersion. The cell volume can also be reduced to less than 300 nL for microbore LC by simple gasket changes.

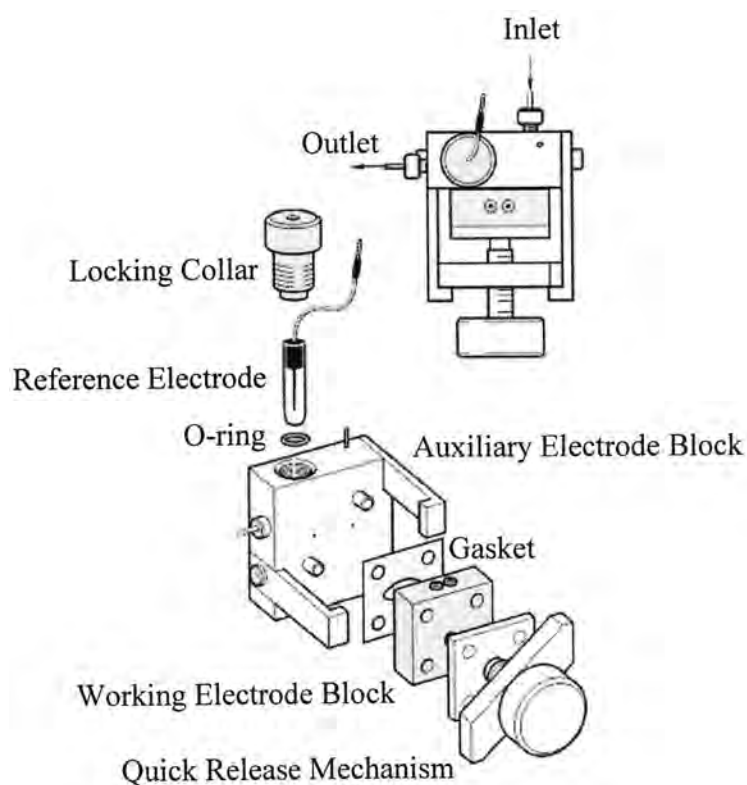


Figure 2.18 Schematic diagram of a thin-layer amperometric flow cell.

2.4 Sample Preparation [60]

Sample preparation is a technique used to clean-up a sample before analyzing and/or to concentrate a sample to improve its detection. The most important problem in analysis is interferences that lead to low sensitivity. Therefore, sample preparation is usually needed to eliminate interferences and to increase the sensitivity. Most samples consist of two distinct parts, the analytes and the matrix. The analytes are the compounds of interest that must be analyzed, while the matrix is the remainder of the sample that does not require analysis. Sample preparation may include dissolving the sample, extracting analyte from a complex matrix, concentrating a dilute analyte to a

level that can be measured, chemically converting analyte into a detectable form, or removing interfering species. The purpose of sample preparation is to have a processed sample that leads to better analytical results compared to those of the initial sample.

2.4.1 Solid-Phase Extraction (SPE) [61,62]

Solid-phase extraction is a technique for sample preparation that concentrates and purifies analytes from solution by sorption onto a disposable solid phase cartridge, followed by elution of the analyte with an appropriate solvent for analysis. A typical solid-phase cartridge is shown in Figure 2.19. SPE techniques have been developed to replace the traditional liquid-liquid extraction methods. The mechanisms of retention include reversed phase, normal phase, and ion exchange. SPE techniques provided a way to perform sample preparation quickly with less solvent and to isolate analytes from large volumes of samples with minimal or no evaporation losses, all while providing good, reproducible results.

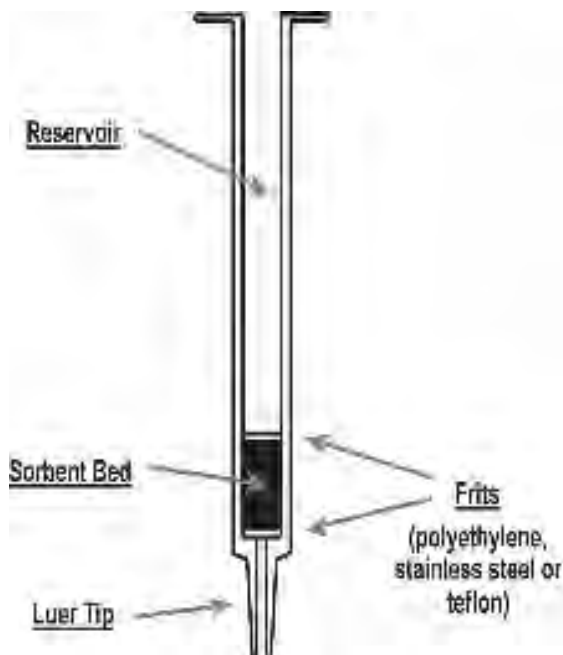


Figure 2.19 Anatomy of a SPE cartridge.

2.4.1.1 Mode of solid-phase extraction [49,51]

2.4.1.1.1 Reversed phase

The interested analytes in this phase are usually moderate to non-polar. The hydrophobic interactions referred to here are non-polar interactions, van-der Waals, or dispersion forces. A secondary interaction between silica and analyte can occur and end capping is useful for reduction of these interactions. However, secondary interactions may be useful in the extraction of highly polar compounds or matrices, as reversed-phase sorbents are packed with more hydrophobic material. The aqueous sample is commonly analyzed by reversed phase SPE. The reversed phase sorbents are non-polar functionalized such as C-18, C-8, C-2, cyclohexyl and phenyl functional groups and bonded to the silica or polymeric sorbent.

2.4.1.1.2 Normal phase

Normal phase SPE refers to the sorption of an analyte by a polar surface and is a standard type of separation. The mechanism for normal phase is polar interactions through hydrogen bonding, dipole-dipole interaction, π - π interaction or induced dipole-dipole interactions. Polar-functionalized bonded silica (LC-CN, LC-NH₂, and LC-Alumina) is typically used in normal phase conditions. For example, the silica base is extremely hydrophilic, so this material adsorbs polar compounds from the non-polar matrix and elutes compounds with a more polar organic solvent than the original sample matrix.

2.4.1.1.3 Ion exchange

Ion exchange can be used for compounds that are charged in solution. Hydrophobic ion exchange is capable of exchanging both cations and anions with free cation or anion functional groups. Strong cation-exchange sorbents consist of interaction sites, like sulfonic acid groups, and weak cation-exchange sites, like carboxylic acid groups. Strong anion-exchange sorbents are quaternary, primary, and secondary amines, while tertiary amines are used for weak ion exchange. The secondary non-polar interaction with non-polar portions can be provided. A decrease

in the balance of pH, ionic strength, and organic content may be necessary for elution of the analyte of interest from these sorbents. While the strong sites are always shown as an exchange site at any pH, weak sites are present only at pH levels greater or less than the pKa. This method has found many applications in natural products, protein, and cellulose analysis, in addition to trace analyte enrichment.

2.4.1.1.4 Mixed mode

The deliberate use of two different functional groups on the same sorbent is called “mixed-mode SPE”. These sorbents are useful for complex samples that differ in polarity and ionization. Mixed-mode sorbents contain co-bonded ion exchange and alkyl group materials. Two different functional groups eliminate the need for a complex sample matrix. The initial hydrophobic interaction is a function of the chain length, with shorter chains (C-4) being retained less than longer chains (C-18). An example of a mixed-mode is shown in Figure 2.20, with reversed phase (hydrocarbon) and cation-exchange sites of the sorbent (amino functional group) drawn.

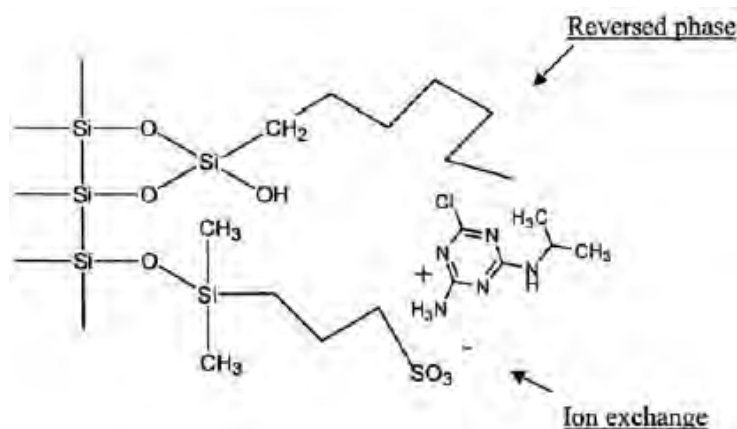


Figure 2.20 Mixed-mode SPE.

Currently, Oasis HLB cartridges are very interesting for sample preparation. This material is a hydrophilic-lipophilic balanced sorbent in SPE that is composed of two monomers (N-vinylpyrrolidone and divinylbenzene). This material has exhibited excellent retention capacity for a wide polarity of analytes. Figure 2.21 shows the structure of the packing material in Oasis HLB cartridges.

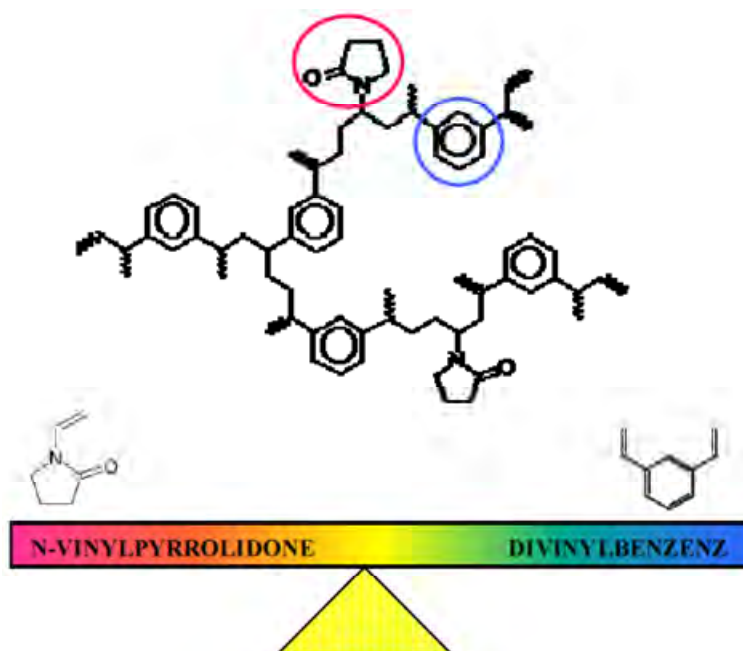


Figure 2.21 Structure of packing material in Oasis HLB cartridges.

2.4.1.2 Steps of solid phase extraction [63]

The SPE process can be divided into four main steps: (1) conditioning, (2) loading, (3) washing, and (4) eluting, illustrated in Figure 2.22.

Step 1, the conditioning step, is the first for the solid-phase sorbent. Before loading of any analytes by the stationary phase can begin, the sorbent bed must be prepared and made compatible with the liquid solution. This simply means that a solvent is passed through the sorbent to wet the packing material and to solvate the functional groups of the sorbent. Furthermore, the air present in the column is removed and the void spaces are filled with solvent. Typically, the conditioning solvent is methanol, which is then followed by water or an aqueous buffer. Following the methanol with by water or buffer activates the column in order for the sorption mechanism to work properly for aqueous samples. Care must be taken not to allow the bonded-silica packing or the polymeric sorbent to go dry. In fact, if the sorbent dries for more than several minutes under vacuum, the sorbent must be reconditioned. If it is not reconditioned, the mechanism of sorption will not work effectively and analyte recoveries will be poor.

In step 2, the sample and analyte are applied to the column, which is called the retention or loading step. Depending on the type of sample, from 1 mL to 1 L of sample may be applied to the column, either by gravity feed, pumping, aspiration by vacuum, or by an automated system. It is important that the mechanism of retention holds the analyte on the column while the sample is added. The mechanisms of retention include van der Waals interactions (also called non-polar, hydrophobic, partitioning, or reversed-phase), hydrogen bonding, dipole-dipole forces, size exclusion, and cation and anion exchange. This retention step is the digital step, or “on/off mechanism”, of solid-phase extraction. During this retention step, the analyte is concentrated on the sorbent. Some of the matrix components may also be retained and others may pass through, which affords some purification of the analyte.

Step 3, the washing step, is used to rinse the column of interfering materials and to retain the analyte. The rinse will remove the sample matrix from the interstitial spaces of the column while retaining the analyte. If the sample matrix is aqueous, an aqueous buffer or a water-organic-solvent mixture may be used. If the sample is dissolved in an organic solvent, the rinse solvent could be the same solvent.

Step 4, the last step, is elution of the analyte from the sorbent with an appropriate solvent that is specifically chosen to disrupt the analyte-sorbent interaction, resulting in elution of the analyte. The eluting solvent should remove as little as possible of the other substances sorbed on the column. This is the basic method of solid-phase extraction, but there is an alternative method where the interference is sorbed and the analytes pass through the column. The analyte is then collected and assayed directly after elution.

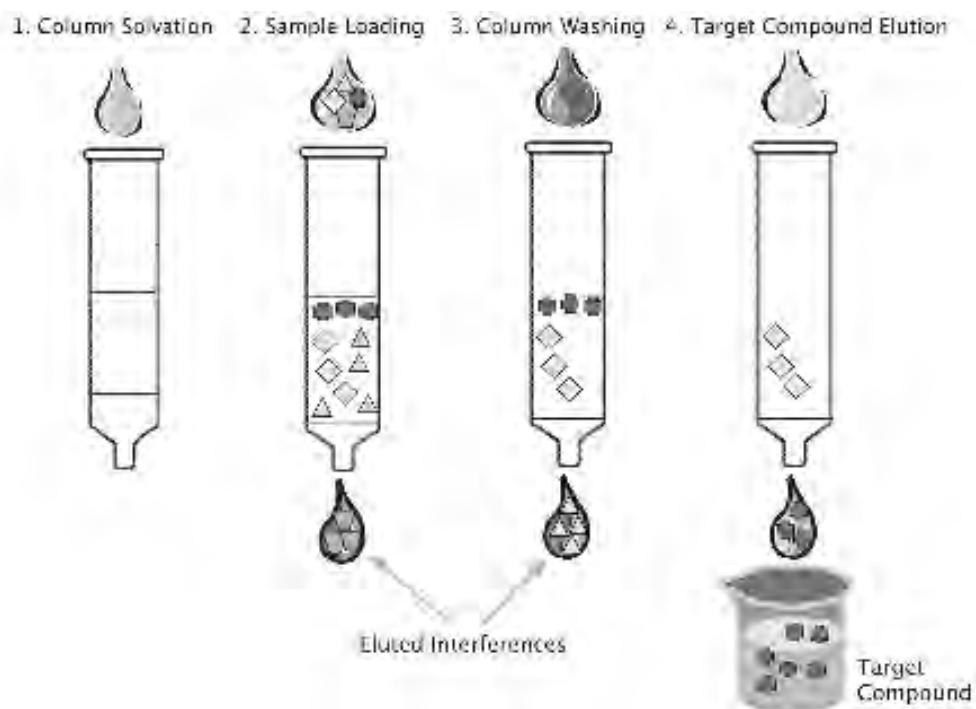


Figure 2.22 The-steps of solid-phase extraction.

CHAPTER III

EXPERIMENTAL

3.1 Chemical and Reagents

- 3.1.1 Sulfadiazine (Sigma-Aldrich)
- 3.1.2 Sulfadimethoxine (Sigma-Aldrich)
- 3.1.3 Sulfaguanidine (ICN Biomedical Inc)
- 3.1.4 Sulfamethazine (Sigma-Aldrich)
- 3.1.5 Sulfamethoxazole (Sigma-Aldrich)
- 3.1.6 Sulfamonomethoxine (Sigma-Aldrich)
- 3.1.7 Sulfaquinoxaline (Sigma-Aldrich)
- 3.1.8 Potassium dihydrogen orthophosphate (BDH)
- 3.1.9 di-sodium hydrogen phosphate dihydrate (Merck)
- 3.1.10 Citric acid (Carlo Erba)
- 3.1.11 Sodium hydroxide (Merck)
- 3.1.12 Ethylenediaminetetraacetic acid disodium salt dehydrate (Sigma-Aldrich)
- 3.1.13 Ethanol (HPLC Grade, Merck)
- 3.1.14 Methanol (HPLC Grade, Merck)
- 3.1.15 Acetonitrile (HPLC Grade, Merck)
- 3.1.16 ortho-phosphoric acid 85% (Merck)
- 3.1.17 A standard buffer solution pH 4 and pH 7 (Metrohm)

3.2 Instruments and Equipment

- 3.2.1 Autolab potentiostat 100 (Eco-chemic, Netherland)
- 3.2.2 CHI1232A (CH Instrument, USA)
- 3.2.3 HPLC compact pump model 2250 (Bischoff, Germany)
- 3.2.4 Eight port selection valve (Hamillton, Nevada, USA)
- 3.2.5 Six port switching valve (Rheodyne MXT 715-000, USA) with a 34 μ L loop (PTFE tubing, 0.5 mm. i.d.)
- 3.2.6 Syringe pump (Hamillton, Nevada, USA)

- 3.2.7 RP-18e monolithic column silica base Chromolith® Performance (100 mm x 4.6 mm i.d., Merck)
- 3.2.8 RP-18e monolithic column silica base Chromolith® guard cartridge kit (5 mm x 4.6 mm i.d., Merck)
- 3.2.9 Electrochemical flow cell (Bioanalytical System Inc., USA)
- 3.2.10 Teflon cell gasket (Bioanalytical System Inc.)
- 3.2.11 PEEK tubing (0.25 mm. i.d.) and connecting (Upchurch)
- 3.2.12 Teflon tubing (1/10 inch i.d., Upchurch)
- 3.2.13 Silver/silver chloride (Ag/AgCl) electrode (Bioanalytical System Inc., USA)
- 3.2.14 Platinum wire (Bioanalytical System Inc., USA)
- 3.2.15 Boron-doped diamond (BDD) electrode (Toyo Kohan Co., Ltd., Japan)
- 3.2.16 Oasis HLB SPE cartridges 200 mg, 6 mL (Water, USA)
- 3.2.17 Mobile phase filter set included 300 mL glass reservoir, glass membrane holder, 1000 mL flask and metal clip (Millipore, USA)
- 3.2.18 Milli Q water system (Millipore, USA, $R \geq 18.2 \text{ M}\Omega\text{cm}$)
- 3.2.19 pH meter (Metrohm 744 pH meter, Metrohm, Switzerland)
- 3.2.20 Analytical balance (Mettler AT 200, Mettler, Switzerland)
- 3.2.21 Ultrasonic bath (ULTRASONIK 28H, ESP Chemicals, Inc., USA)
- 3.2.22 Centrifuge (Beckman Coulter, USA)
- 3.2.23 Vortex mixer (Mixer Uzusio LMS. Co. Ltd., Japan)
- 3.2.24 Autopipette and tips (Eppendorf, Germany)
- 3.2.25 Filters membrane (0.2 μM , 47 mm, Whatman)
- 3.2.26 Nylon Syringe filters (0.45 μm , 13 mm, Chromex)
- 3.2.27 Nylon Syringe filters (0.20 μm , 13 mm, Chromex)
- 3.2.28 Vacuum pump (GAST, USA)
- 3.2.29 Beaker 10, 25, 50, 100, 250, 500 and 1,000 mL
- 3.2.30 Volumetric flask 5,10, 25, 50, 500 and 1,000 mL

3.3 Preparation of solutions

3.3.1 Preparation of solution in Cyclic Voltammetry

3.3.1.1 Standard Stock Solutions

Each standard stock solution (10 mM) of seven sulfonamides was prepared by weighing SQ 0.032 g, SDM 0.031 g, SDZ 0.025 g, SG 0.021 g, SMM 0.028 g, SMX 0.025 g and SMZ 0.028 g, dissolved each sulfonamides with acetonitrile: Milli Q water (50: 50; v/v), and then transferred each sulfonamides into 10.00 mL volumetric flask. All of the standard solution were stored at 4 °C in amber glass and protected from the light.

3.3.1.2 Supporting Electrolyte

The phosphate buffer solution at pH 3 was prepared by dissolving potassium dihydrogen phosphate 0.8982 g with 100 mL of Milli-Q water and then transferred into a 100 mL volumetric flask. The pH was adjusted with phosphoric acid and 0.1 M sodium hydroxide.

3.3.1.3 Working Standard Solution

The volume of electrochemical cell for cyclic voltammetry is 3 mL. The concentrations were prepared by pipetting of each standard stock solution 10 mM into electrochemical cell and adjusted to 3 mL with supporting electrolyte. The concentration and volumes required for preparations are shown in Table 3.1.

Table 3.1 Composition of each concentration for seven sulfonamides in electrochemical cell for cyclic voltammetry.

Final concentration of each sulfonamide standard solution (mM)	Volume of stock solution (μL)	Volume of supporting electrolyte (μL)
0.10	30	2,970
0.25	75	2,925
0.50	150	2,850
0.75	225	2,775
1.00	300	2,700

3.3.2 Preparation of solution for HPLC-EC

3.3.2.1 Standard Stock Solution

A standard stock solution ($500 \mu\text{g mL}^{-1}$) of each sulfonamide was prepared by dissolving 5 mg of sulfonamide with acetonitrile: Milli Q water (50: 50; v/v) in 10.00 mL volumetric flask and stored at 4 °C in the dark.

A standard stock solution of seven sulfonamides mixture ($500 \mu\text{g mL}^{-1}$) was prepared by dissolving 5 mg of SQ, SDM, SDZ, SG, SMM, SMX and SMZ with acetonitrile: Milli Q water (50: 50; v/v) in 10.00 mL volumetric flask and stored at 4 °C in the dark.

The mixed working standard solution was prepared by dilution of the standard stock solution with the mobile phase.

3.3.2.2 Mobile phase

0.05 M phosphate buffer solution (pH 3) was prepared daily by dissolving 6.8 g of potassium dihydrogen phosphate in 1,000 mL volumetric flask with Milli Q

water and adjusted pH by phosphoric acid. The mobile phase for HPLC consisted of the phosphate buffer solution, acetonitrile and ethanol in the ratio of 80: 15: 5 (v/v/v). All solutions and solvents were filtered through 0.45 μm Nylon membranes and degassed by ultrasonic bath.

3.3.3 Preparation of solution for Sample Preparation

3.3.3.1 Na₂EDTA-MacIlvaine's Buffer Solution

Na₂EDTA-MacIlvaine's buffer was the extraction solution. The Na₂EDTA-MacIlvaine's buffer pH 4 was prepared by weighing of 1.352 g citric acid, 1.302 g disodium hydrogen phosphate dehydrate and 0.372 g ethylenediaminetetraacetic acid disodium salt dehydrate, dissolved with Milli Q water. After that the mixture was transferred into 100 mL volumetric flask.

3.3.4 Preparation of SPE column

Polytetrafluoroethylene (PTFE) tubing (40 mm in length \times 1.59 mm in inner diameter) was used as column blanks for a homemade cylinder microcolumn SPE. The cylinder microcolumn were prepared by filling 60 mg of Oasis HLB (particle size 30 μm) into the PEEK tubing, as above, using the wet packing method. The slurry was prepared from 1 g of Oasis HLB in 3 mL of methanol. To avoid loss of Oasis HLB when the sample solution passes through the cylinder microcolumn, polyethylene frits was placed at both of ends of the microcolumn. The preparation of SPE microcolumn is shown in Figure 3.1. The microcolumn SPE was used for the sample clean-up and extraction of sulfonamides in solution.

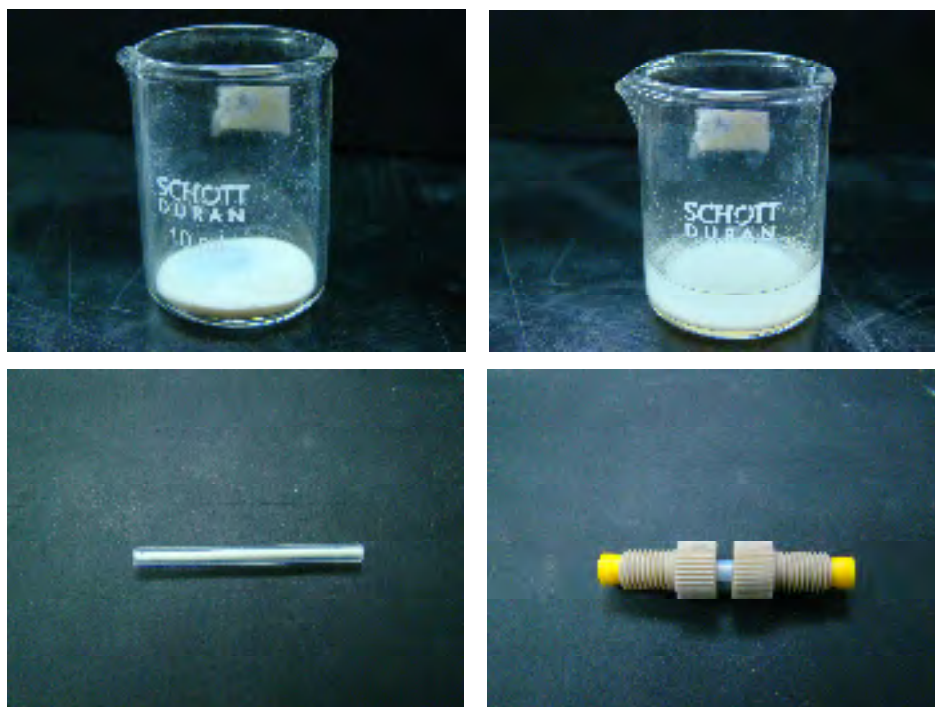


Figure 3.1 The preparation of SPE microcolumn.

3.3.5 Preparation of Sample

The real samples were fresh shrimp in local supermarket. One gram of a homogeneous shrimp sample was placed in a 15 mL amber glass bottle, and 5 mL of Na_2EDTA –McIlvaine’s buffer solution was added into the bottle. The mixture was well mixed on a vortex mixer for 5 min at high speed. After that, the mixture was placed in an ultrasonic water bath for 10 min following centrifugation at 20,000 rpm for 10 min. The collected supernatant was cleaned up and extracted with automated on-line SPE microcolumn. Prior to load supernatant into SPE microcolumn, they were filtered through a 0.20 μm Nylon membrane filter.

3.4 Procedure

3.4.1 Cyclic Voltammetry

Cyclic voltammetric investigations of the electrochemical behaviors of seven sulfonamides were studied in a electrochemical cell, with a volume of 3 mL. The

cyclic voltammetry measurements were performed in a single-compartment, three-electrode glass cell as illustrated in Figure 3.2. An Ag/AgCl with a salt bridge, a platinum wire and a BDD electrode were used as the reference electrode, the counter electrode and the working electrode, respectively. The BDD electrode was pressed at the bottom of the cell, and isolated by placing the backside of the Si substrate onto a brass plate. The BDD electrode was sonicated with Milli Q water prior to use. The electrochemical equipment was housed in a faradaic cage to reduce electronic noise. The voltammograms were recorded using an autolab potentiostat 100.



Figure 3.2 The electrochemical cell for cyclic voltammetry experiment.

3.4.1.1 The Scan Rate Dependence Study

The effect of the scan rate on the electrochemical behaviors of sulfonamides was investigated by variation of the scan rate in cyclic voltammetry. The solutions of 0.5 mM SQ, SDM, SDZ, SG, SMM, SMX and SMZ in 0.05 mM phosphate buffer solution (pH 3) were prepared. The potential was scanned from 0.5-1.4 V at the scan rate of 10, 25, 100, 150 and 200 mV s^{-1} . The peak currents obtained from cyclic voltammogram at each scan rate were plotted as a function of the square root of the scan rate.

CHAPTER IV

RESULTS AND DISCUSSION

4.1 Cyclic Voltammetric Investigation

The electrooxidation of seven SAs was investigated by cyclic voltammetry. This technique was used to study the electrochemical characteristics of SQ, SDM, SDZ, SG, SMM, SMX, and SMZ. A platinum wire as the counter electrode, Ag/AgCl as the reference electrode and BDD as the working electrode were all used for cyclic voltammetry in this report. The cyclic voltammograms for 0.1 mM standard solutions of SQ, SDM, SDZ, SG, SMM, SMX, and SMZ in phosphate buffer solution (pH3) are shown in Figure 4.1. The reaction obtained was observed on the positive scan from 0.5 to 1.4 V versus Ag/AgCl at a scan rate of 50 mV s⁻¹. The potential of seven sulfonamides are shown in Table 4.1.

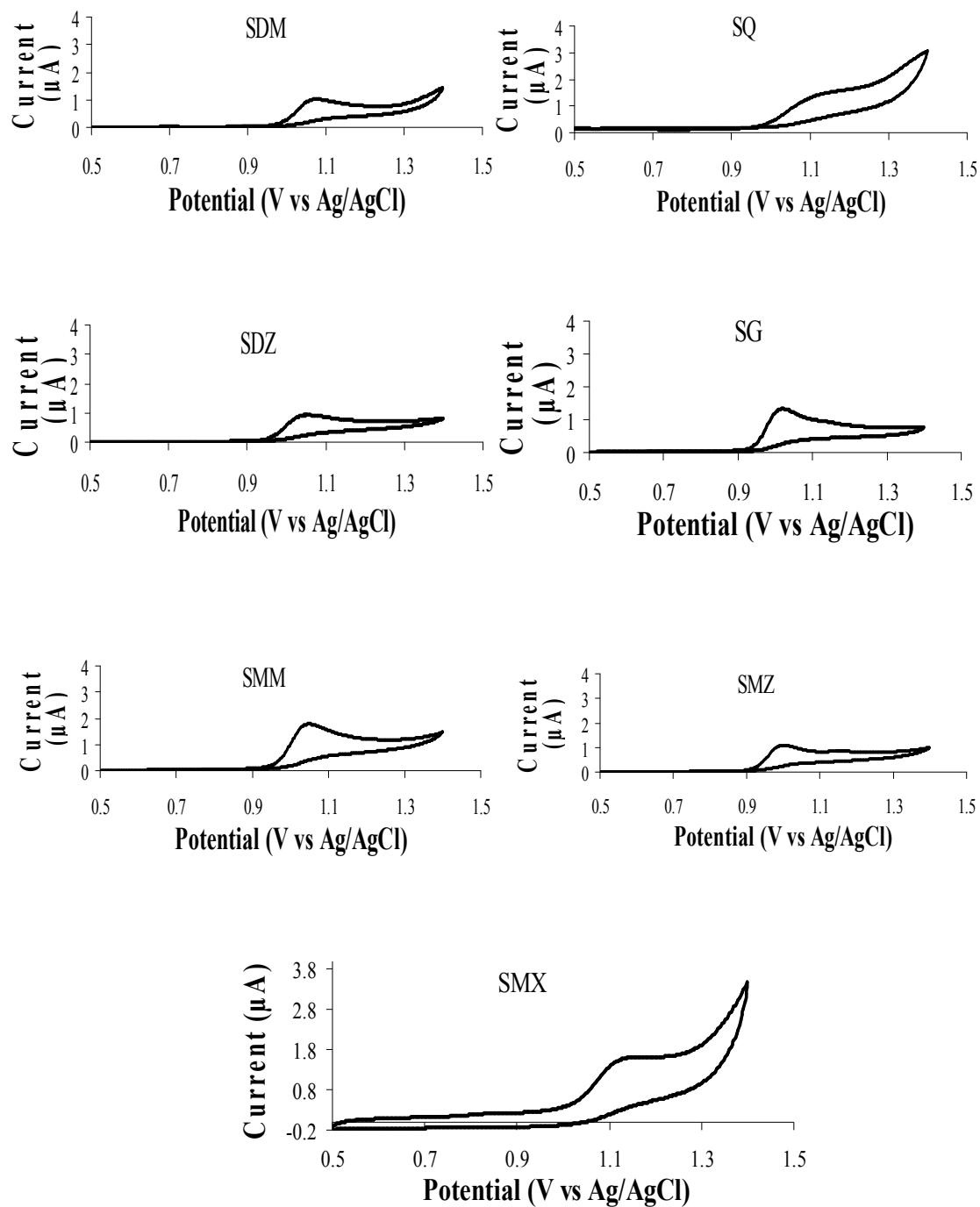


Figure 4.1 Cyclic voltammograms for 0.1 mM standard solutions of SQ, SDM, SDZ, SG, SMM, SMX, and SMZ in phosphate buffer solution (pH 3) at a BDD electrode. The scan rate was 50 mV s⁻¹.

Table 4.1 Potentials of 0.1 mM SAs in 0.05 M phosphate solution (pH 3) with a scan rate of 50 mV s⁻¹ at a BDD electrode.

Sulfonamide	Potential of SAs (V vs. Ag/AgCl)
Sulfaquinoxaline (SQ)	1.135
Sulfadimethoxine (SDM)	1.068
Sulfadiazine (SDZ)	1.044
Sulfaguanidine (SG)	1.019
Sulfamethazine (SMM)	1.046
Sulfamethoxazole (SMX)	1.129
Sulfamethazine (SMZ)	0.998

4.1.1 Scan Rate Dependence Study

The effect of the scan rate on the electrochemical behaviors of SG, SDZ, SMZ, SMM, SMX, SDM, and SQ were investigated by variation of the scan rate from 10 to 200 mV s⁻¹. The relationship between the current responses versus the square root of the scan rate ($v^{1/2}$) was highly linear ($R^2 > 0.99$) for the seven SAs, as shown in the insets of Figures 4.2 through 4.8, respectively. It can be seen that the current response is directly proportional to the square root of the scan rate. From these results, it can be concluded that the diffusion process controls the transportation of these analytes.

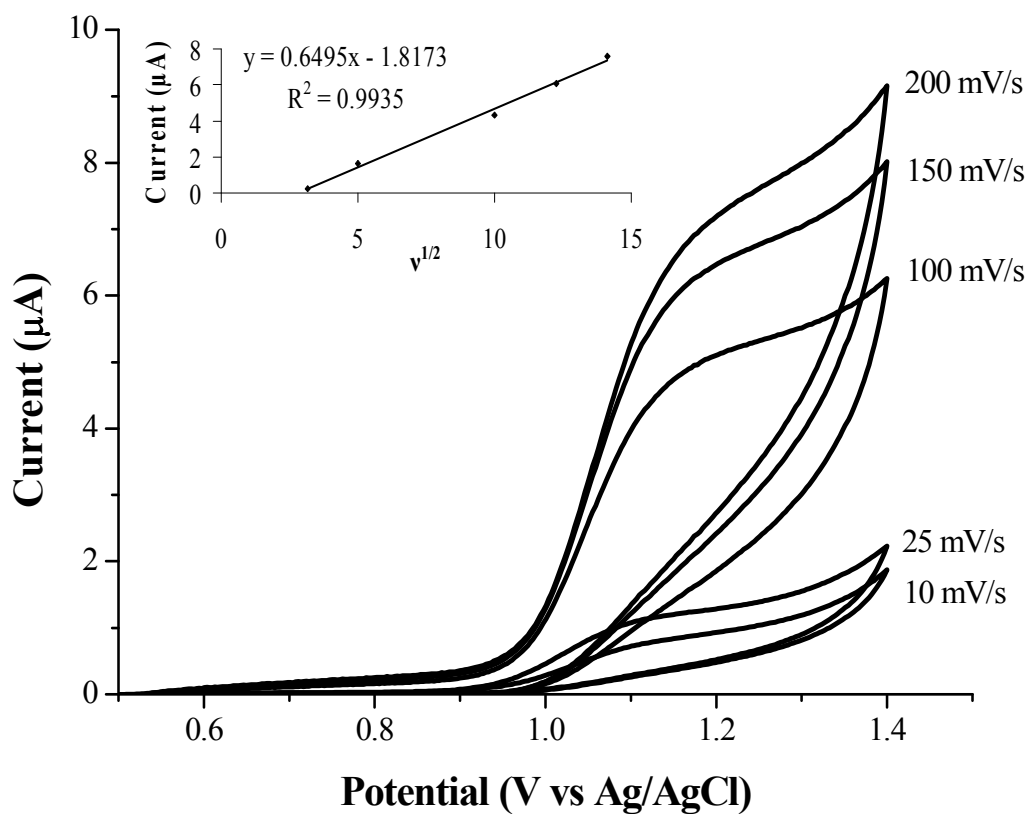


Figure 4.2 Cyclic voltammograms for 0.5 mM SG in phosphate buffer solution (pH 3) at a BDD electrode. The scan rate was varied from 10 to 200 mV s^{-1} . Inset shows the relationship of the current response versus the square root of the scan rate ($v^{1/2}$).

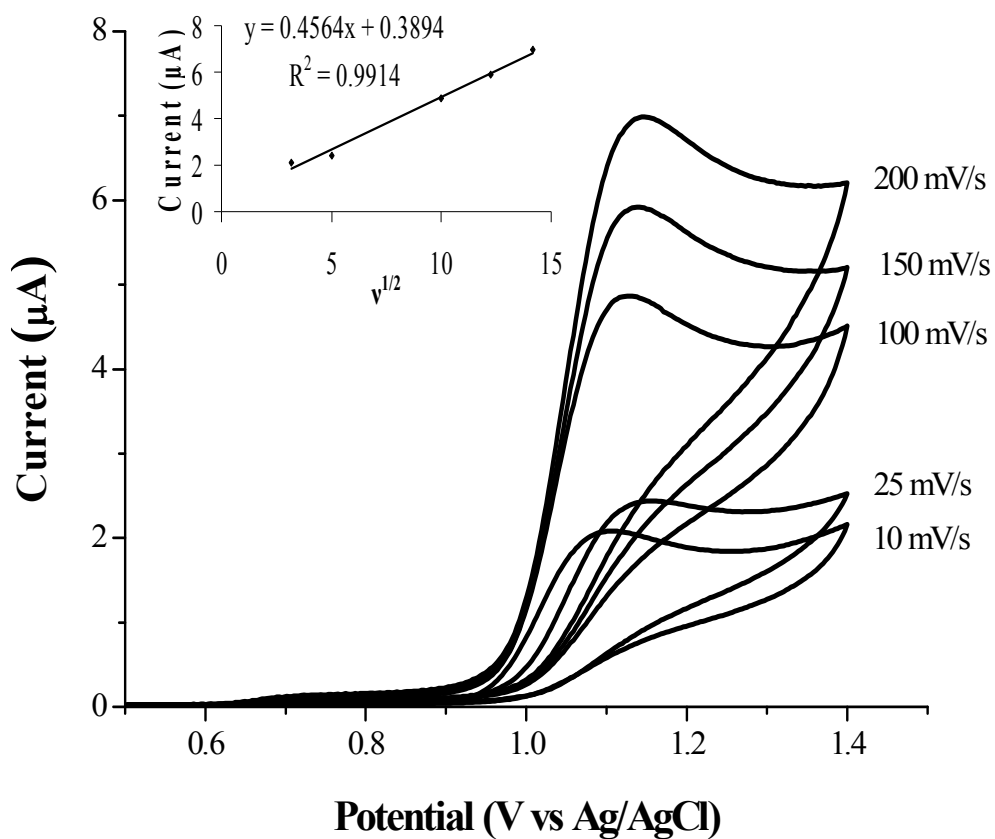


Figure 4.3 Cyclic voltammograms for 0.5 mM SDZ in phosphate buffer solution (pH 3) at a BDD electrode. The scan rate was varied from 10 to 200 mV s^{-1} . Inset shows the relationship of the current response versus the square root of the scan rate ($v^{1/2}$).

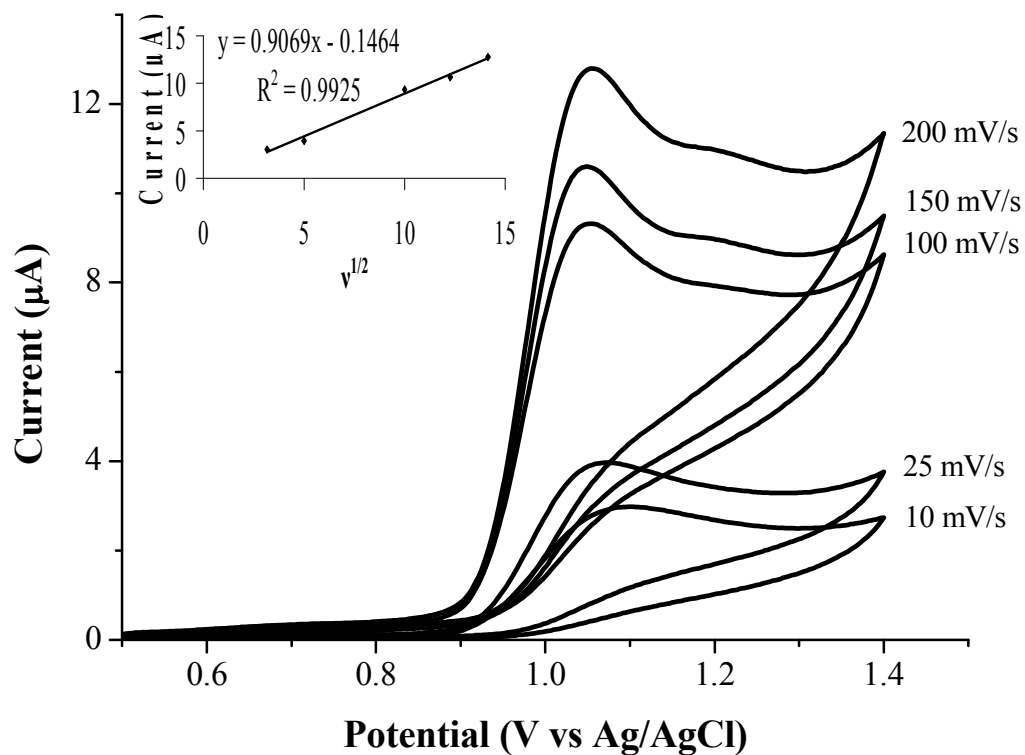


Figure 4.4 Cyclic voltammograms for 0.5 mM SMZ in phosphate buffer solution (pH 3) at a BDD electrode. The scan rate was varied from 10 to 200 mV s^{-1} . Inset shows the relationship of the current response versus the square root of the scan rate ($v^{1/2}$).

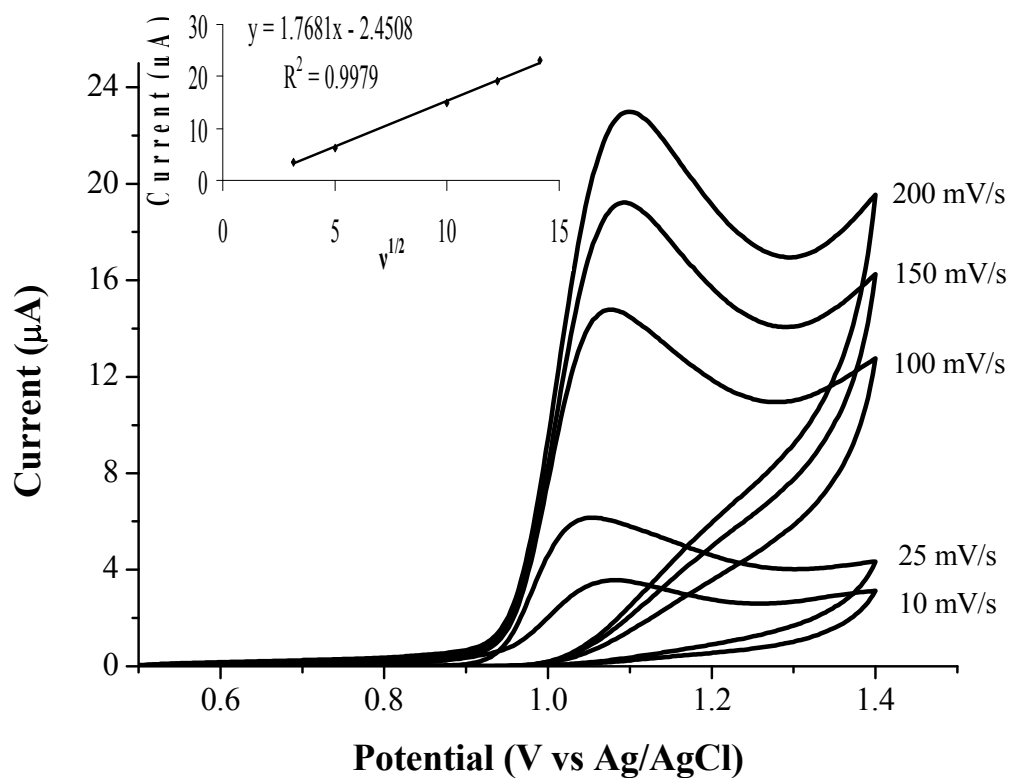


Figure 4.5 Cyclic voltammograms for 0.5 mM SMM in phosphate buffer solution (pH 3) at a BDD electrode. The scan rate was varied from 10 to 200 mV s^{-1} . Inset shows the relationship of the current response versus the square root of the scan rate ($v^{1/2}$).

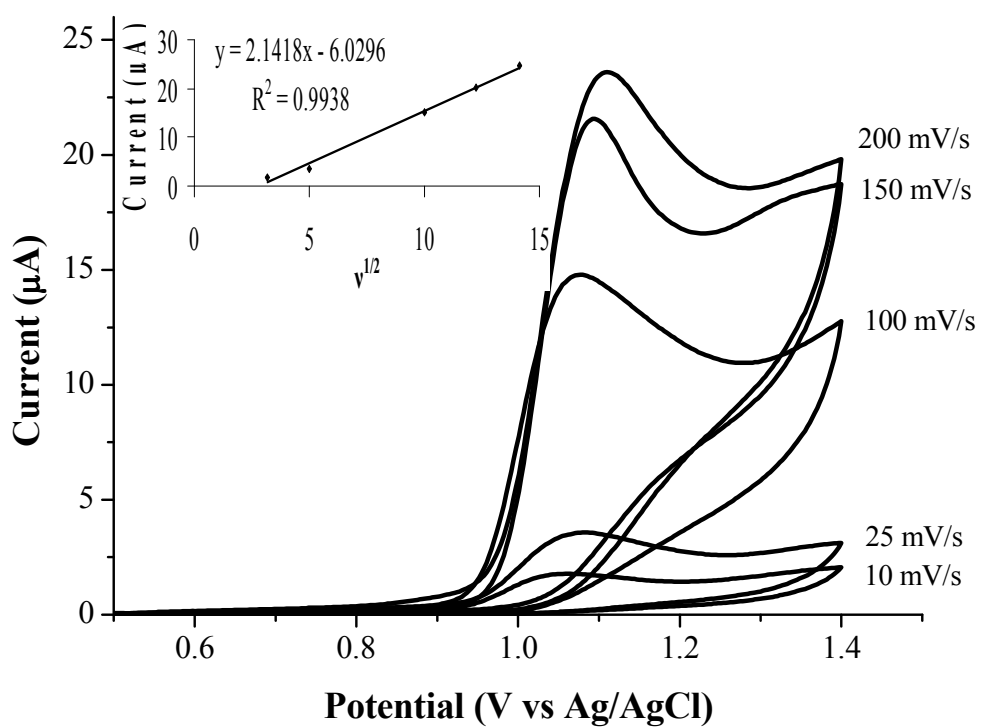


Figure 4.6 Cyclic voltammograms for 0.5 mM SMX in phosphate buffer solution (pH 3) at a BDD electrode. The scan rate was varied from 10 to 200 mV s^{-1} . Inset shows the relationship of the current response versus the square root of the scan rate ($v^{1/2}$).

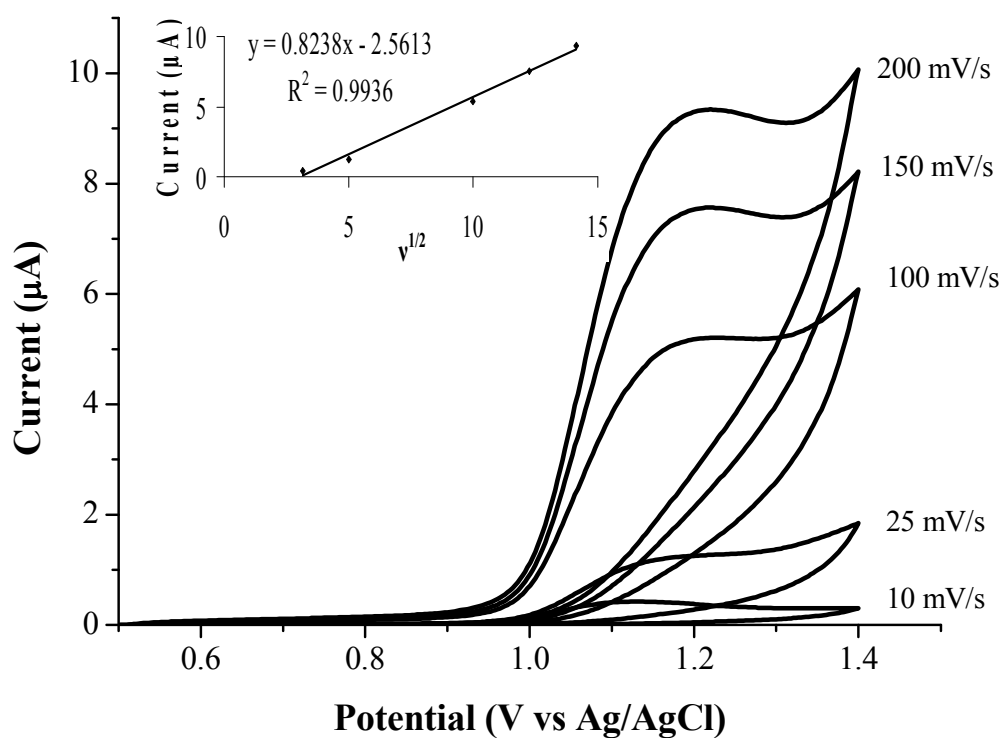


Figure 4.7 Cyclic voltammograms for 0.5 mM SDM in phosphate buffer solution (pH 3) at a BDD electrode. The scan rate was varied from 10 to 200 mV s^{-1} . Inset shows the relationship of the current response versus the square root of the scan rate ($v^{1/2}$).

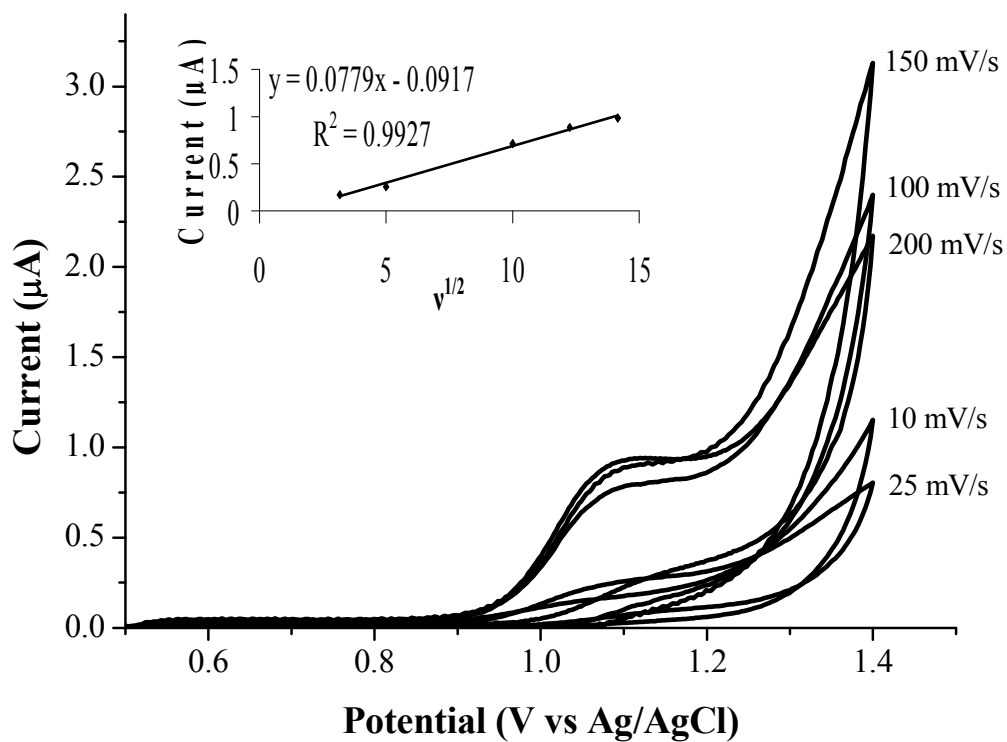


Figure 4.8 Cyclic voltammograms for 0.5 mM SQ in phosphate buffer solution (pH 3) at a BDD electrode. The scan rate was varied from 10 to 200 mV s^{-1} . Inset shows the relationship of the current response versus the square root of the scan rate ($v^{1/2}$).

4.1.2 Concentration Dependence Study

The relation between voltammetric responses and the concentration of SG, SDZ, SMZ, SMM, SMX, SDM, and SQ were investigated by varying the concentrations of these analytes from 0.1 to 1 mM. The results are shown in Figures 4.9 through 4.15. It was found from this study that the peak current increased with increasing concentrations of the seven SAs. The peak current was linearly proportional to the concentration ranging from 0.1 to 1 mM. Linear regression analysis of these data yielded a $R^2 > 0.99$.

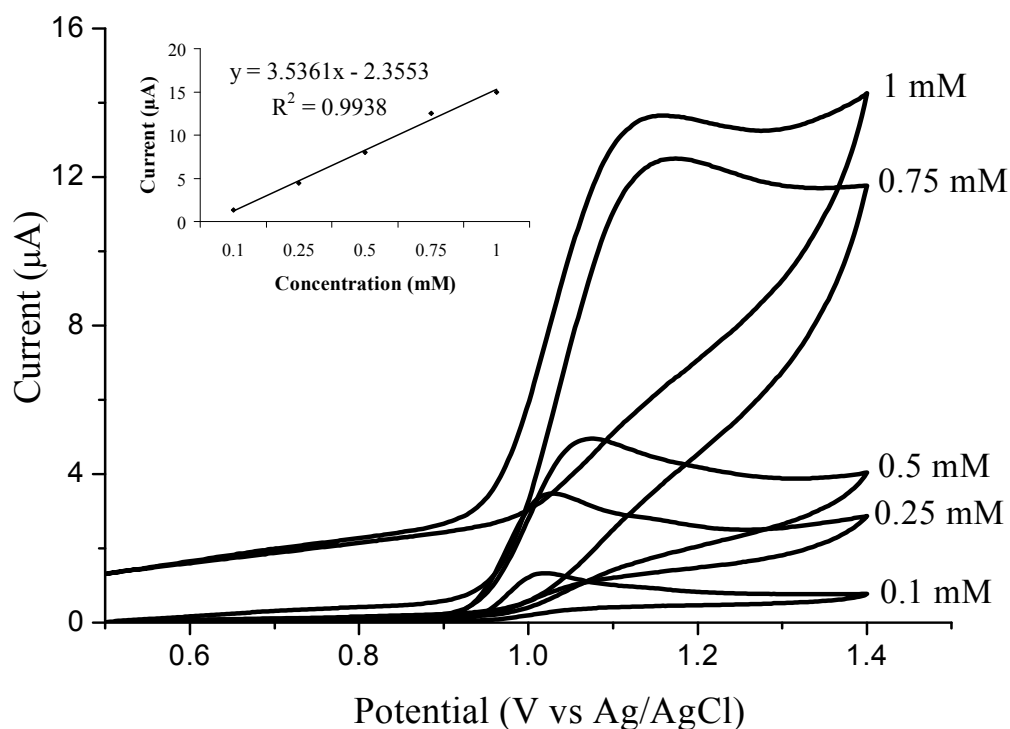


Figure 4.9 Cyclic voltammograms of SG in phosphate buffer solution (pH 3) at a BDD electrode. The concentration was increased from 0.1 to 1 mM. Inset shows the relationship of the current response against the concentration.

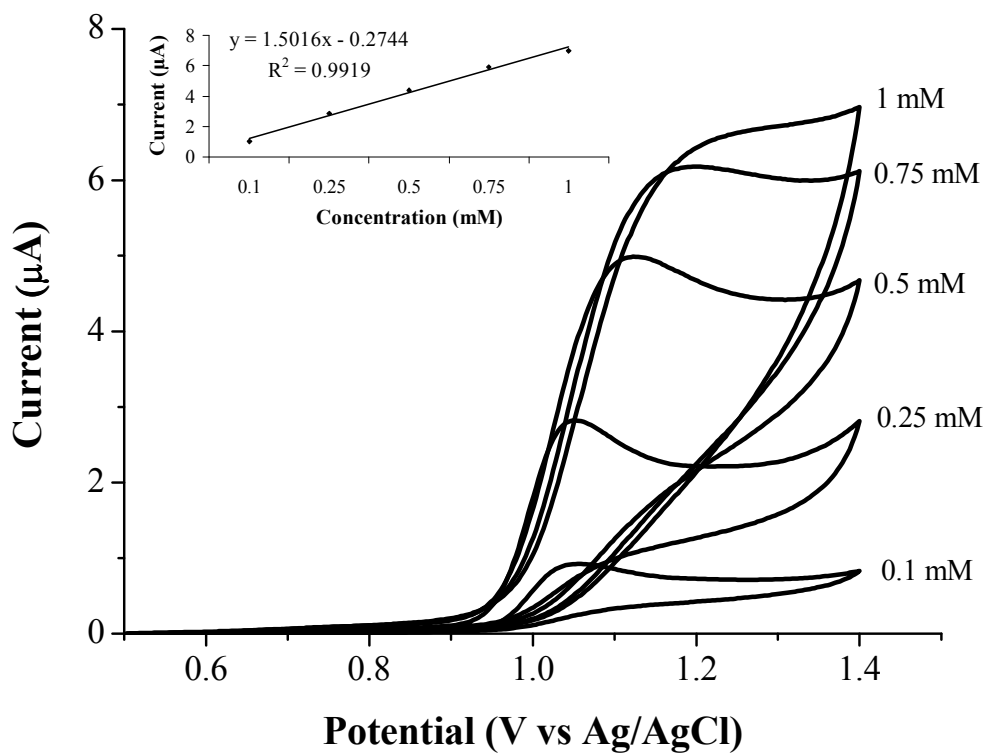


Figure 4.10 Cyclic voltammograms of SDZ in phosphate buffer solution (pH 3) at a BDD electrode. The concentration was increased from 0.1 to 1 mM. Inset shows the relationship of the current response against the concentration.

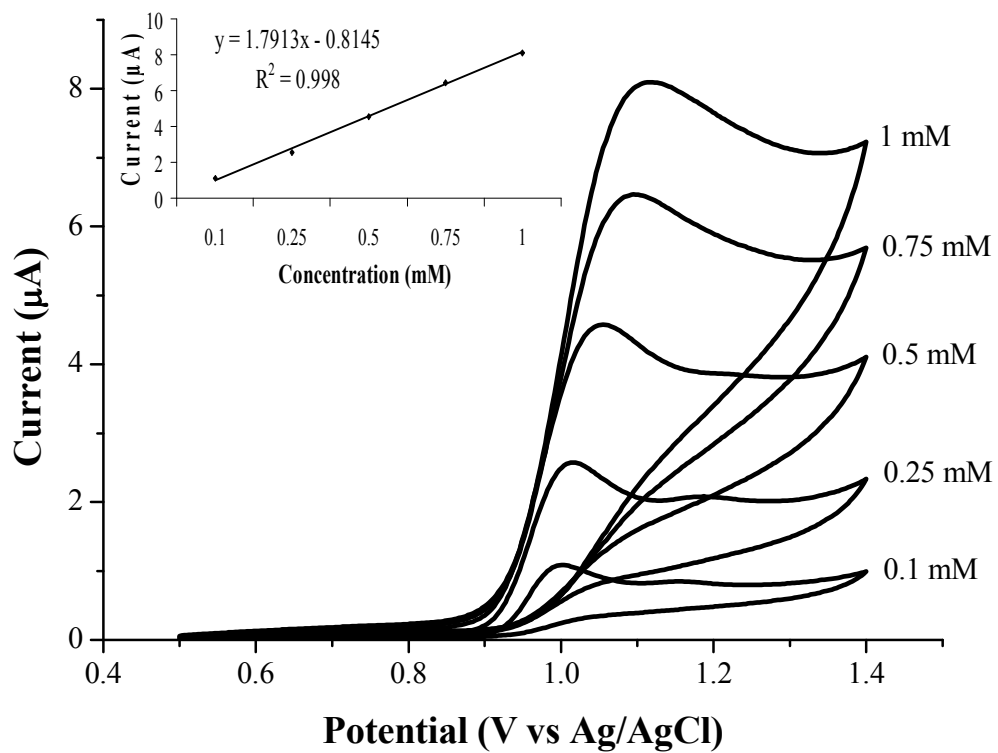


Figure 4.11 Cyclic voltammograms of SMZ in phosphate buffer solution (pH 3) at a BDD electrode. The concentration was increased from 0.1 to 1 mM. Inset shows the relationship of the current response against the concentration.

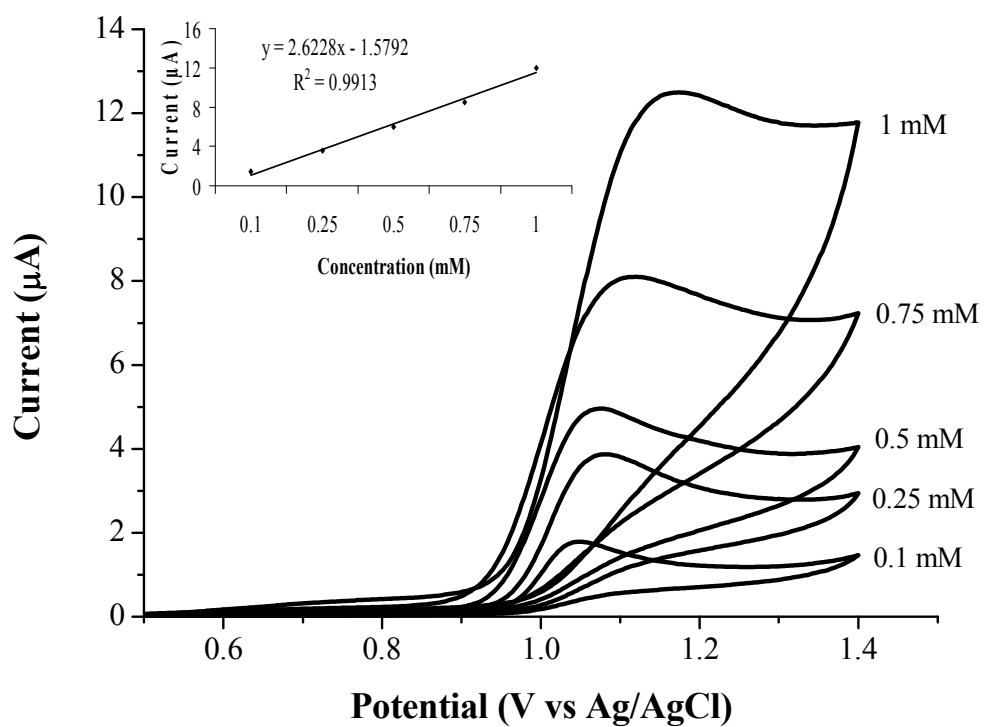


Figure 4.12 Cyclic voltammograms of SMM in phosphate buffer solution (pH 3) at a BDD electrode. The concentration was increased from 0.1 to 1 mM. Inset shows the relationship of the current response against the concentration.

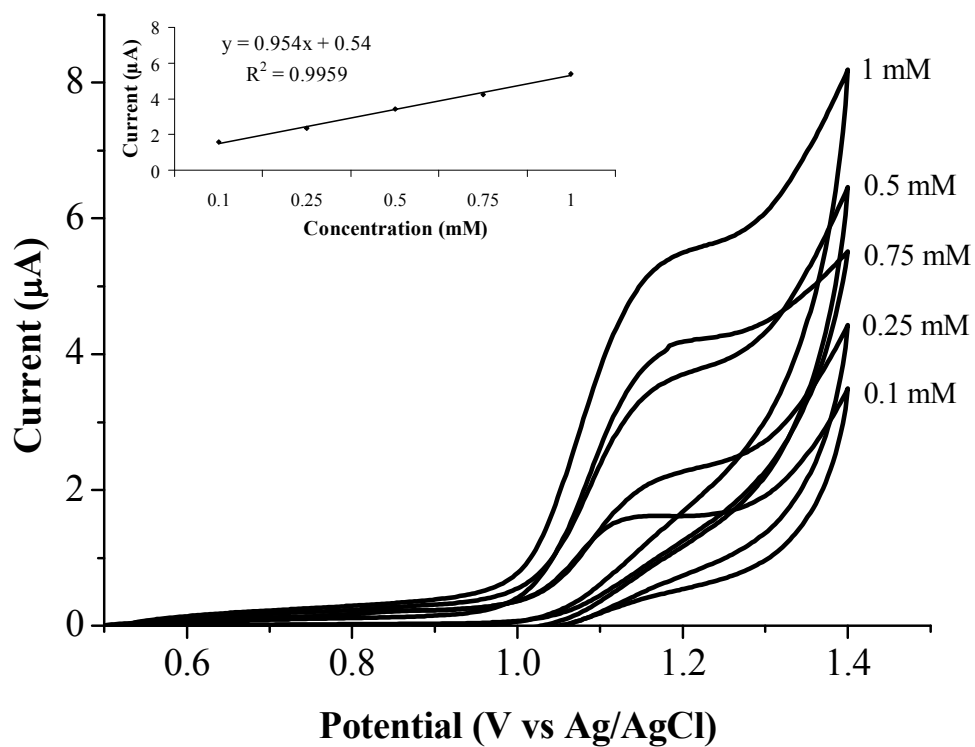


Figure 4.13 Cyclic voltammograms of SMX in phosphate buffer solution (pH 3) at a BDD electrode. The concentration was increased from 0.1 to 1 mM. Inset shows the relationship of the current response against the concentration.

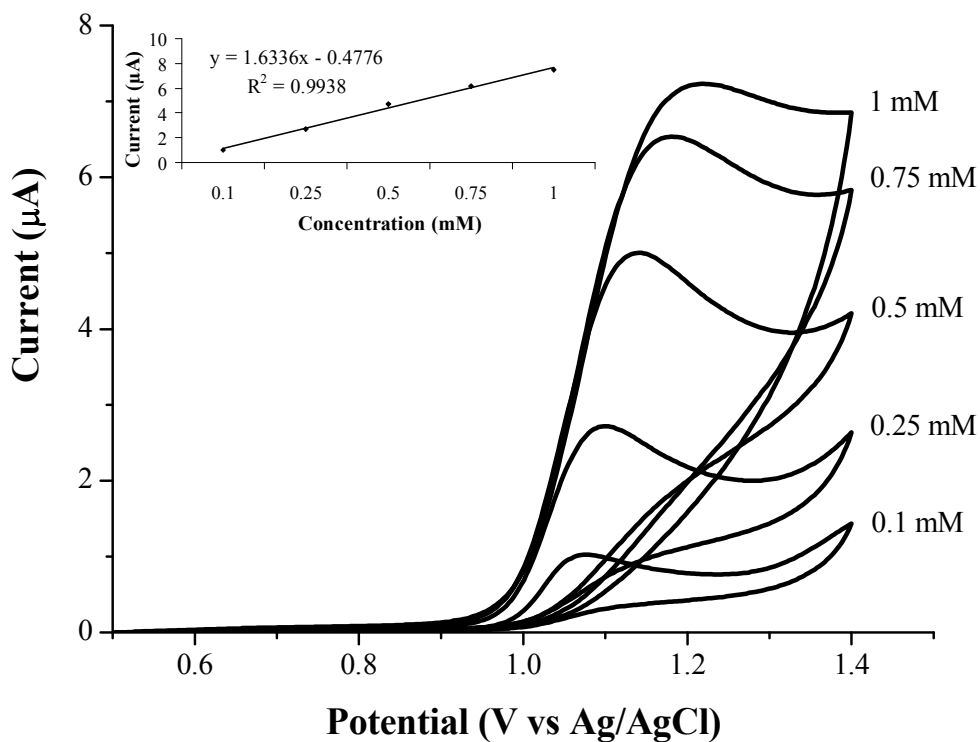


Figure 4.14 Cyclic voltammograms of SDM in phosphate buffer solution (pH 3) at a BDD electrode. The concentration was increased from 0.1 to 1 mM. Inset shows the relationship of the current response against the concentration.

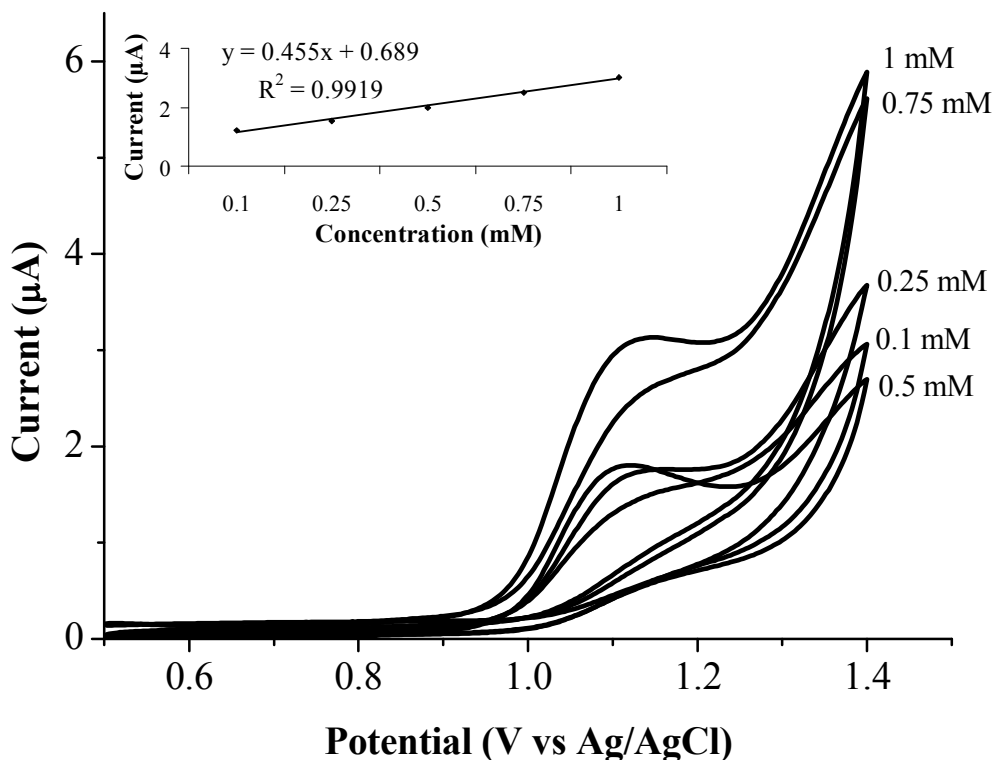


Figure 4.15 Cyclic voltammograms of SQ in phosphate buffer solution (pH 3) at a BDD electrode. The concentration was increased from 0.1 to 1 mM. Inset shows the relationship of the current response against the concentration.

4.2 Optimal Conditions of HPLC-EC

The conditions for HPLC-EC analysis of seven SAs was investigated from previously published results [64]. The optimal conditions (Table 3.3) were applied to the separation of SG, SDZ, SMZ, SMM, SMX, SDM, and SQ. The analysis time for separation was less than 10 min in all cases. Figure 4.16 shows the chromatogram for the separation of a standard solution of the seven SAs studied in this report. The retention times for SG, SDZ, SMZ, SMM, SMX, SDM, and SQ were 2.73, 3.11, 3.67, 4.46, 5.26, 8.52 and 9.33 min, respectively.

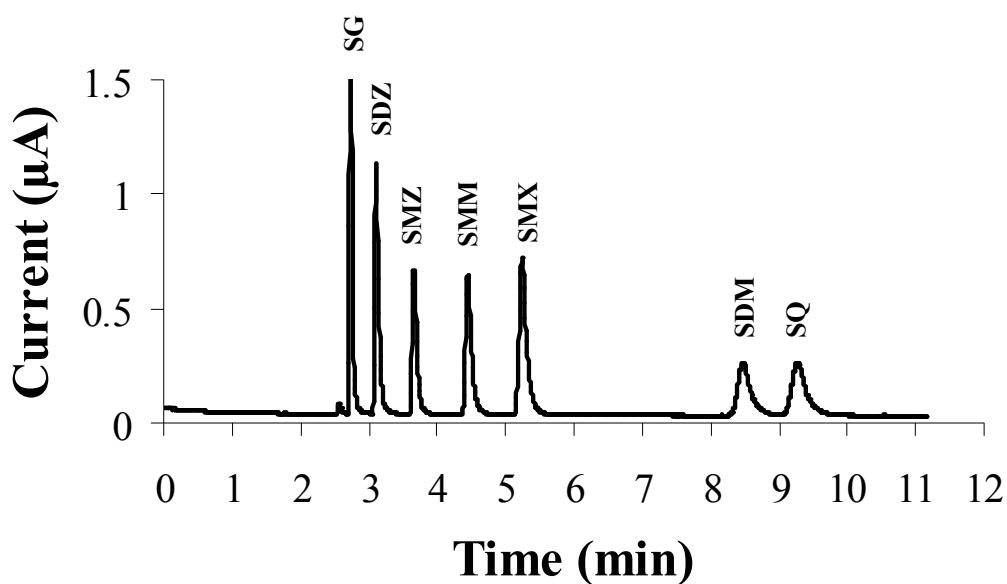


Figure 4.16 HPLC-EC chromatogram of a $10 \mu\text{g mL}^{-1}$ mixture of seven standard SAs separated on a monolithic column at a flow rate of 1.5 mL min^{-1} . The detection potential was $1.2 \text{ V vs. Ag/AgCl}$ using a BDD electrode.

4.3 On-line SPE-HPLC-EC

4.3.1 Effect of eluent

The optimal ratio of eluent (methanol) to mobile phase (phosphate buffer: acetonitrile: ethanol) was studied across 50:50, 60:40, 70:30, 80:20, 90:10, and 100:0 (v/v) ratios. The peak areas for seven sulfonamides were found to increase with increasing methanol ratio. A compromise between good resolution and high sensitivity, an eluent of 100% methanol was selected, because this condition can be used to separate seven sulfonamides. Moreover, the sensitivity of SDM and SQ are higher than those obtained from other conditions, as shown in Figure 4.17.

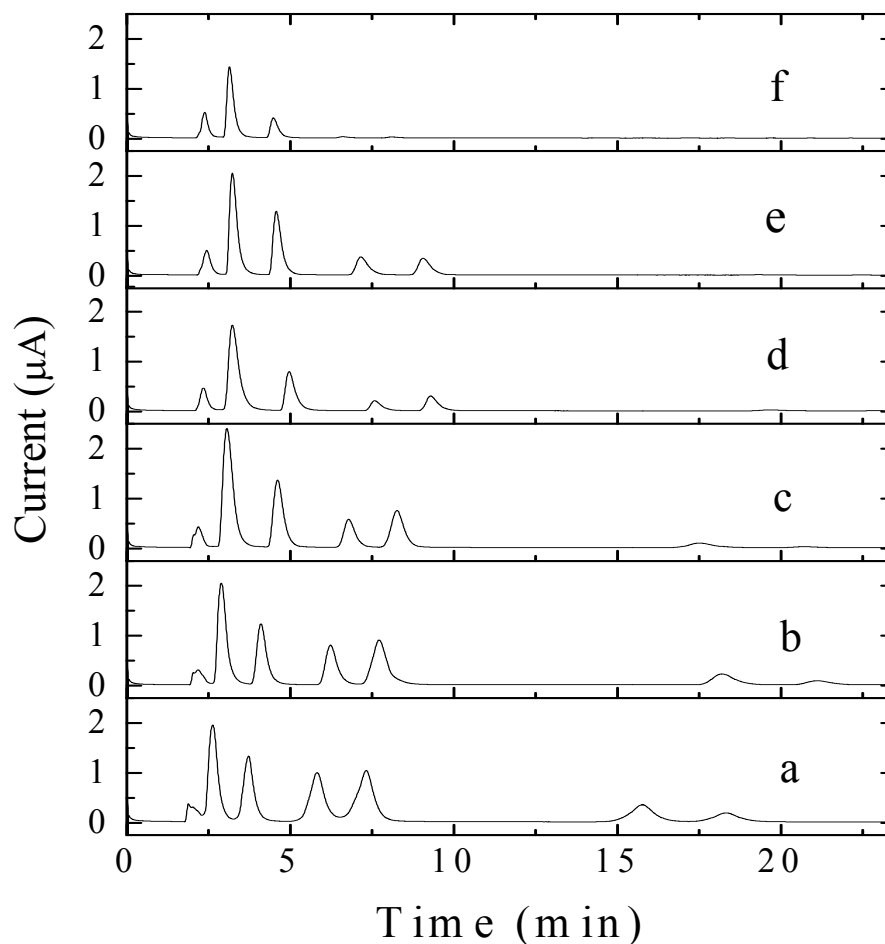


Figure 4.17 HPLC chromatograms of sulfonamides ($10 \mu\text{g mL}^{-1}$) at different ratios of eluent and mobile phase. (a) methanol, (b) methanol: mobile phase 90:10, (c) 80:20, (d) 70:30, (e) 60:40, (f) 50:50.

4.3.2 Effects of sample loading and elution rate

The flow rate will influence on the retention of sulfonamides on the SPE column. The sample loading and elution rate was studied at 8, 9, 10, and $11 \mu\text{L s}^{-1}$. Figure 4.18 shows that the peak current of the seven sulfonamides increase when the sample loading and elution rate increase up to $10 \mu\text{L s}^{-1}$. The peak current decrease when the sample loading and elution rate is higher than $10 \mu\text{L s}^{-1}$ because the high flow rate effects on the interaction between analyte and sorbent in SPE column. Therefore, the band broadening occur at the lower flow rate. Furthermore, the resolution of the seven sulfonamides was not affected by changing the flow rate.

Therefore, the sample loading and elution rate of $10 \mu\text{L s}^{-1}$ was selected as optimal value.

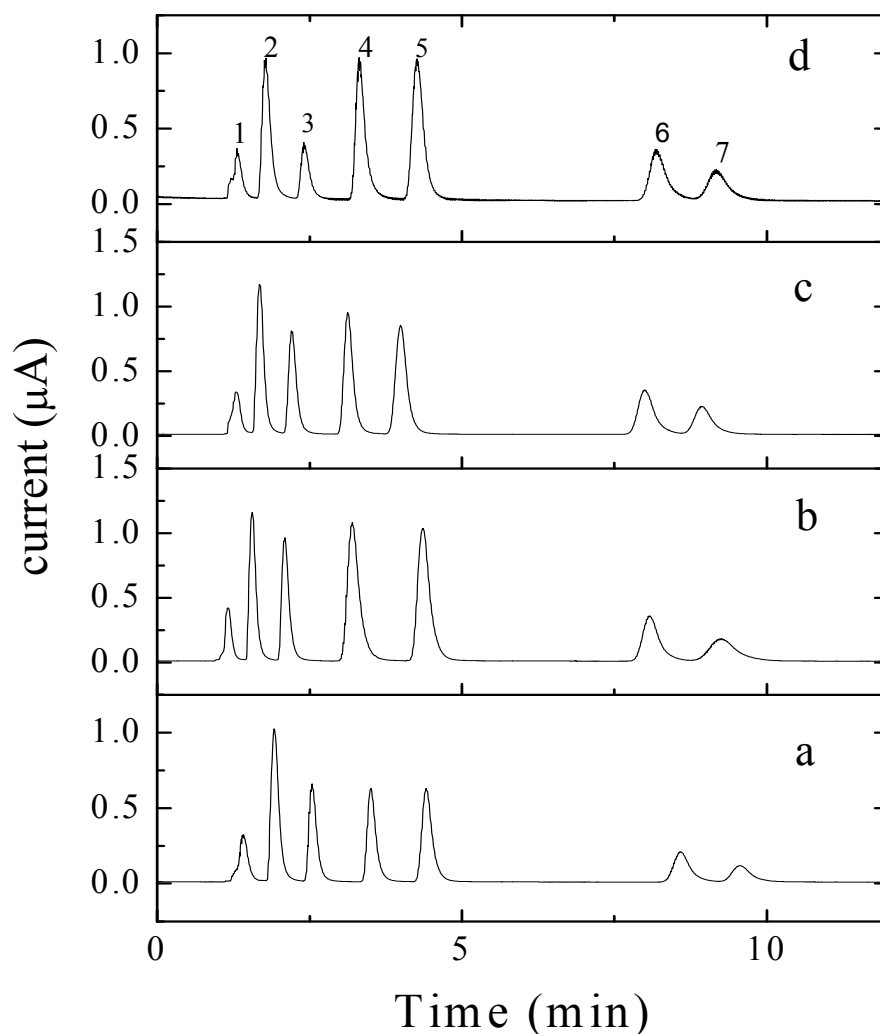


Figure 4.18 HPLC chromatograms of seven sulfonamides ($10 \mu\text{g mL}^{-1}$); (1) sulfaguanidine, (2) sulfadiazine, (3) sulfamethazine, (4) sulfamonomethoxine, (5) sulfamethoxazole, (6) sulfadimethoxine, (7) sulfaquinoxaline at different sample loading flow rates and eluting flow rates. (a) $11 \mu\text{L s}^{-1}$, (b) $10 \mu\text{L s}^{-1}$, (c) $9 \mu\text{L s}^{-1}$, (d) $8 \mu\text{L s}^{-1}$.

4.3.3 Effect of eluate zone

The effect of the eluate zone was also studied at 20-24, 25-29, and 30-34 s. The results are shown in Figure 4.19, where elution zone is represented by elution time. Elution time was calculated from the start to the stop of the elution step. It was found that peak current for the seven sulfonamides decreased with increasing of the elution time. Hence, the optimal condition selected was 20-24 s for the following experiment.

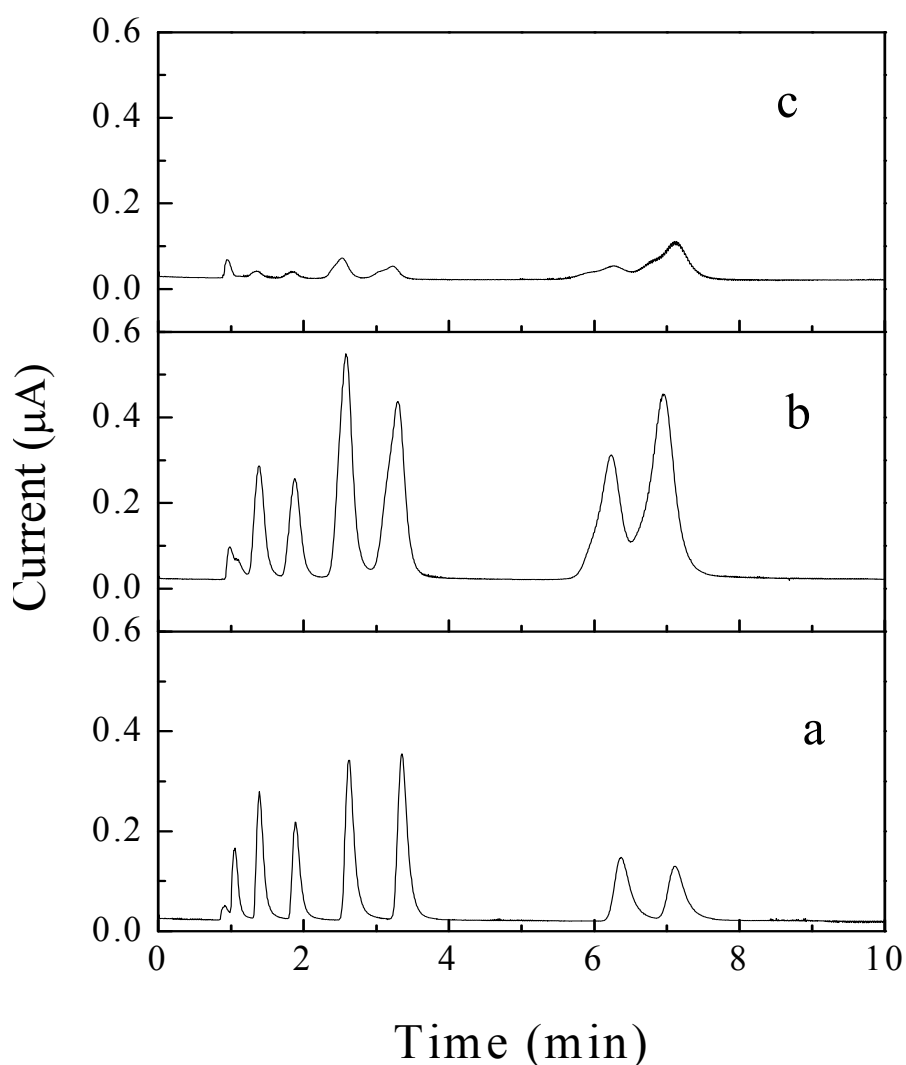


Figure 4.19 HPLC chromatograms of sulfonamides at different zones of eluate. (a) a zone of eluate at time 20-24 s, (b) a zone of eluate at time 25-29 s, (c) a zone of eluate at time 30-34 s.

4.3.4 Calibration and linearity

From the determined optimal conditions, the calibration of the peak areas against concentrations was plotted. The linearities for all of the SAs were within a range between 0.01 to 10 $\mu\text{g mL}^{-1}$. These calibration curves of the seven SAs are shown in Figure 4.20. Each point of the calibration graph corresponds to the mean value from three replicate injections. The slope and y-axis intercept, together with the coefficient of each SA, are shown in Table 4.2.

Table 4.2 Linearity, limit of detection and limit of quantitation of SAs of this method

Analyte	Linearity ($\mu\text{g/mL}$)	Slope (peak area units /ppm)	Intercept (μA)	R ²
SG	0.01-8	0.5277	0.1085	0.9943
SDZ	0.01-8	7.6757	0.0403	0.9982
SMZ	0.01-8	6.5834	0.0769	0.999
SMM	0.01-8	5.2178	0.3764	0.9965
SMX	0.01-8	2.4536	0.0679	0.9994
SDM	0.1-8	2.397	0.2668	0.9957
SQ	0.1-8	0.8786	0.0419	0.9997

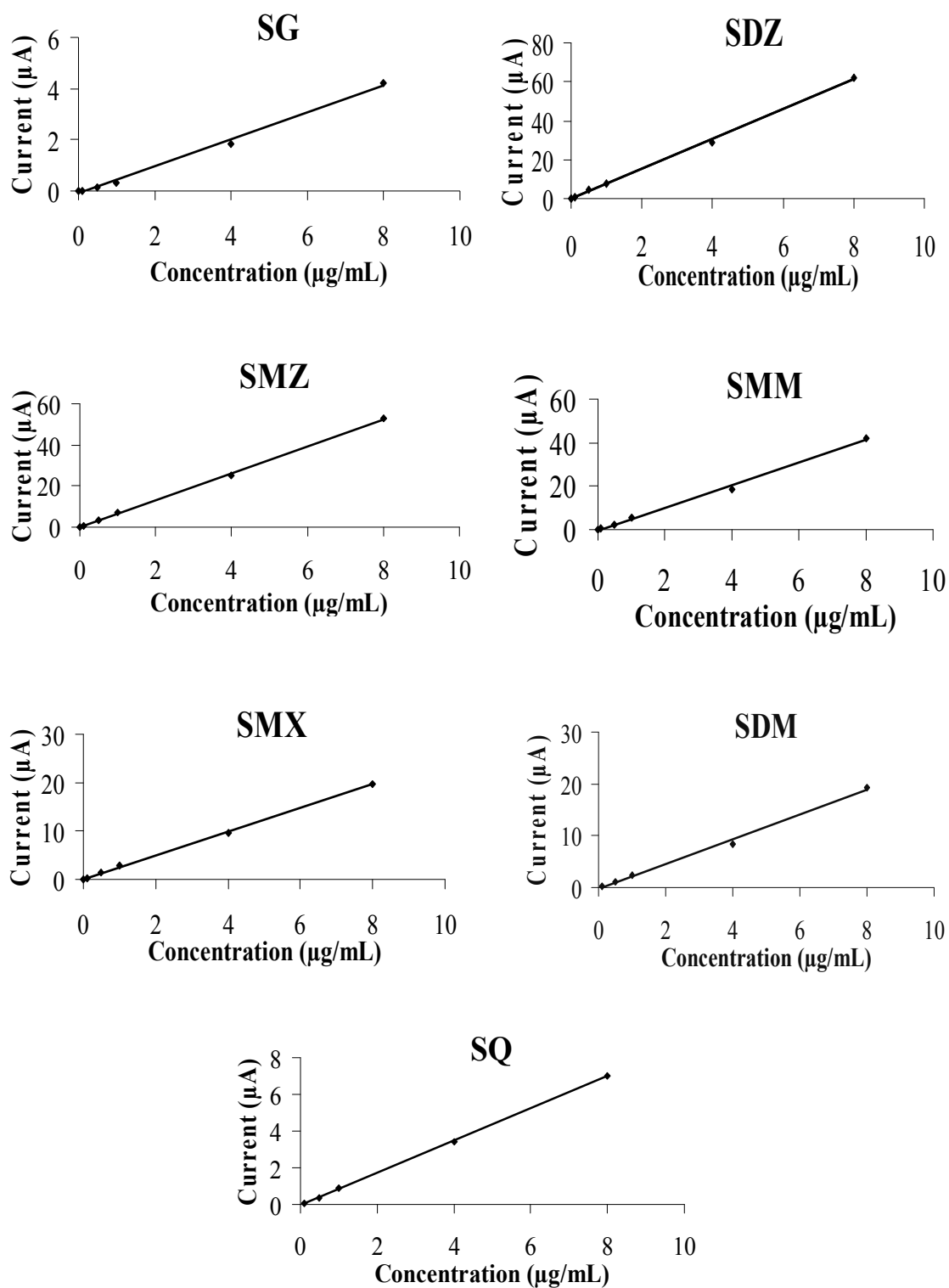


Figure 4.20 Linearity of seven standard SAs by HPLC-EC using a BDD electrode.

4.3.5 LOD and LOQ

The detection limit was investigated by examining various concentrations of SAs from 0.01 to 10 $\mu\text{g mL}^{-1}$. The LOD is defined as the concentration that provides a signal-to-noise ratio of 3 (3S/B). The LOQ was determined under the definition of being ten times the signal-to-noise ratio (10S/B). The slope of the linearity was obtained from Table 4.2 and the LOD and LOQ are summarized in Table 4.3.

Table 4.3 LOD and LOQ of seven standard SAs.

Analyte	LOD (ng mL^{-1})	LOQ (ng mL^{-1})
Sulfaguanidine	11.2	33.6
Sulfadiazine	1.2	4.0
Sulfamethazine	1.3	4.2
Sulfamonomethoxine	1.5	5.0
Sulfamethoxazole	2.9	9.8
Sulfadimethoxine	3.1	10.3
Sulfaquinoxaline	7.4	24.6

4.4 Application to Real Samples

The optimal conditions for on-line SPE-HPLC-EC were applied to the determination of SG, SDZ, SMZ, SMM, SMX, SDM, and SQ in shrimp. The Na_2EDTA -MacIlvaine's buffer solution (pH4) was used to extract SAs from shrimp and an Oasis HLB SPE cartridge was used to clean-up the sample.

4.4.1 Determination of SAs in shrimp

To estimate the applicability of the proposed method, shrimp samples from local supermarkets were investigated by the method of standard addition. The typical chromatogram of a blank shrimp extract and a shrimp extract spiked at 6 $\mu\text{g mL}^{-1}$ are illustrated in Figure 4.21. This method can be used to determine SMZ, SMM, SMX, SDM, and SQ, but SG and SDZ overlapped with interfering compound. This observation could be explained by the fact that protein and lipid content in the shrimp

were very high despite the use of Na_2EDTA -MacIlvaine's buffer solution and SPE for sample preparation.

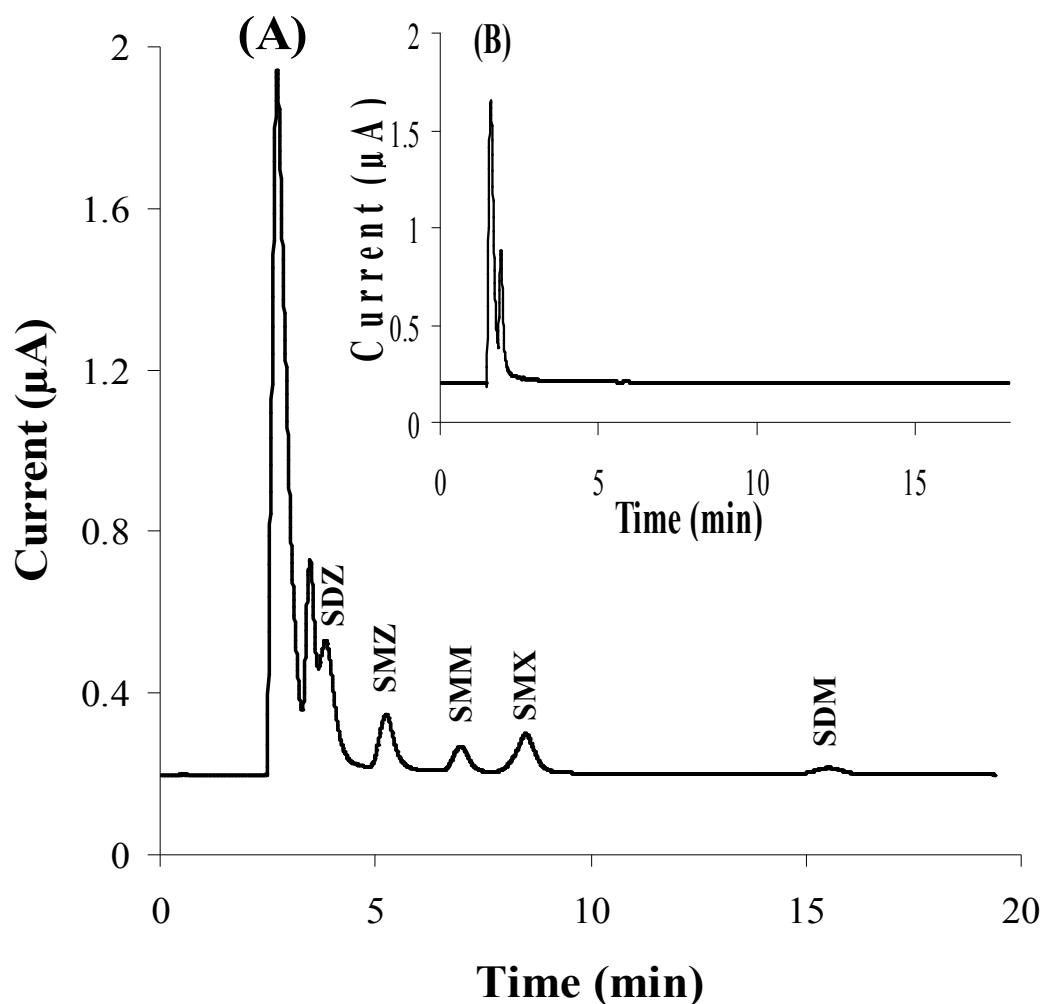


Figure 4.21 On-line SPE-HPLC-EC chromatogram of (A) a shrimp sample spiked with $6 \mu\text{g mL}^{-1}$ of a standard mixture of seven SAs; (B) a blank shrimp sample separated on a monolithic column at a flow rate 1.5 mL min^{-1} . The detection potential was $1.2 \text{ V vs. Ag/AgCl}$ using a BDD electrode.

4.4.2 Accuracy and Precision

The accuracy of the method presented here was calculated from the percent recovery of spiked blank shrimp at 2, 4 and 6 $\mu\text{g mL}^{-1}$. These three concentrations of SAs were representative of the low, medium, and high levels investigated. The precision of the method was calculated by determining the relative standard deviation of the repeated injections of solution containing the complete set of standard compounds. To appraise the repeatability of the analytical process, three concentrations (2, 4 and 6 $\mu\text{g mL}^{-1}$) were studied. The results of intra-day analysis were obtained and repeated in one day. The results of inter-day analysis were obtained and repeatedly analyzed on three different days. The intra- and inter-day precision and recovery of the method are shown in Table 4.4 and Table 4.5, respectively. It was found that the average recoveries ranged from 74.7 – 110.5 % for shrimp. The results obtained from these studies indicated that the method developed in this research provided good accuracy and precision. The recovery and %RSD values were acceptable according to the AOAC manual for the Peer Verified Methods Program that recommended the acceptable recovery and %RSD values for method development (in Appendix).

Table 4.4 Intra-day precisions and recoveries of spiked level 2, 4, and 6 $\mu\text{g mL}^{-1}$.

Analyte	Spiked level ($\mu\text{g mL}^{-1}$)	Recovery of Intra-day (%)				
		1	2	3	mean \pm SD ^a	R.S.D (%)
SMZ	2	77.7	76.8	69.6	74.7 \pm 4.4	5.9
	4	104.1	109.2	105.4	106.2 \pm 2.7	2.5
	6	99.8	97.5	102.8	100.0 \pm 2.7	2.6
SMM	2	90.9	90.6	88.1	89.9 \pm 1.5	1.7
	4	89.2	100.6	97.0	95.6 \pm 5.8	6.1
	6	104.2	101.1	100.4	101.9 \pm 2.1	2.0
SMX	2	95.5	99.0	96.5	97.0 \pm 1.8	0.0
	4	101.2	106.7	81.9	96.6 \pm 13.0	0.1
	6	103.3	108.8	104.5	105.5 \pm 2.9	0.0
SDM	2	117.0	121.3	93.2	110.5 \pm 15.1	13.7
	4	86.4	87.9	87.9	87.4 \pm 0.9	1.0
	6	105.2	102.4	104.3	103.9 \pm 1.4	1.4
SQ	2	85.9	86.0	75.5	82.5 \pm 6.1	7.4
	4	104.1	99.4	103.5	102.4 \pm 2.6	2.5
	6	94.7	100.0	105.6	100.1 \pm 5.4	5.4

^a mean of recovery (%) \pm standard deviation of triplicate measurements.

Table 4.5 Inter-day precisions and recoveries of spiked level 2, 4, and 6 $\mu\text{g mL}^{-1}$.

Analyte	Spiked level ($\mu\text{g mL}^{-1}$)	Recovery of Inter-day (%)				
		1	2	3	mean \pm SD ^a	R.S.D (%)
SMZ	2	83.7	93.1	74.7	83.8 \pm 9.2	10.9
	4	98.5	76.4	106.2	93.7 \pm 15.5	16.5
	6	81.8	97.7	100.0	93.2 \pm 9.9	10.6
SMM	2	107.2	112.1	89.9	103.1 \pm 11.7	11.3
	4	81.1	76.8	95.6	84.5 \pm 9.9	11.6
	6	93.1	120.5	101.9	105.2 \pm 13.9	13.3
SMX	2	86.3	98.7	97.0	94.0 \pm 6.7	7.2
	4	64.1	64.1	96.6	74.9 \pm 18.8	25.0
	6	86.1	101.5	105.5	97.7 \pm 10.2	10.4
SDM	2	84.7	108.6	110.5	101.3 \pm 14.4	14.2
	4	87.7	84.2	87.4	86.4 \pm 1.9	2.2
	6	93.9	111.3	103.9	103.0 \pm 8.7	8.5
SQ	2	113.9	104.8	82.5	100.4 \pm 16.2	16.1
	4	107.6	81.5	102.4	97.2 \pm 13.8	14.2
	6	105.9	111.9	100.1	105.9 \pm 5.9	5.6

^a mean of recovery (%) \pm standard deviation of triplicate measurements.

4.4.3 Comparison of Methods between HPLC-EC and HPLC-MS

The results of the proposed method were compared to those of HPLC-MS from LCFA. Three shrimp samples (blank shrimp, shrimp spiked with SAs at 2 and 6 $\mu\text{g g}^{-1}$) containing SAs were determined for comparison of the two methods. The results obtained by both methods are shown in Table 4.6.

Table 4.6 Comparisons results of two methods in shrimp sample.

Analyte	Concentration of SAs found ^a	
	HPLC-EC	HPLC-MS ^b
Blank shrimp		
SMZ	ND ^c	ND ^c
SMM	ND ^c	ND ^c
SMX	ND ^c	ND ^c
SDM	ND ^c	ND ^c
SQ	ND ^c	ND ^c
Spiking at level 2 $\mu\text{g g}^{-1}$		
SMZ	1.49 \pm 0.08	1.77 \pm 0.10
SMM	1.79 \pm 0.03	1.82 \pm 0.11
SMX	1.94 \pm 0.03	2.04 \pm 0.11
SDM	2.21 \pm 0.30	1.70 \pm 0.09
SQ	1.65 \pm 0.12	1.49 \pm 0.09
Spiking at level 6 $\mu\text{g g}^{-1}$		
SMZ	6.00 \pm 0.15	6.56 \pm 0.18
SMM	6.11 \pm 0.12	6.30 \pm 0.18
SMX	6.33 \pm 0.17	6.61 \pm 0.18
SDM	6.24 \pm 0.09	6.02 \pm 0.17
SQ	6.00 \pm 0.33	5.79 \pm 0.15

^a Mean \pm standard deviation (n=3)

^b Result of Laboratory Center for Food and Agricultural product Company Limited (LCFA)

^c Not detected

CHAPTER V

CONCLUSIONS

5.1 Conclusions

A new method, on-line solid phase extraction (SPE) coupled with sequential injection analysis, was developed for the separation and determination of seven sulfonamides (sulfaguanidine, sulfadiazine, sulfamethazine, sulfamonomethoxine, sulfamethoxazole, sulfadimethoxine, and sulfaquinoxaline) in shrimp samples. The investigation for electroanalysis started with cyclic voltammetry, which showed the irreversible oxidation peak of seven SAs at a BDD electrode. A silica-based monolithic column was used for the separation of sulfonamides because of its high tolerance to organic solvents, which led to a longer lifetime, and low backpressure relative to traditional columns. The methodology was applied to determine residual concentration of the seven sulfonamides in shrimp using an Oasis HLB cartridge for sample extraction. The optimal HPLC conditions were found to be a mobile phase of 0.05 M phosphate buffer (pH3): acetonitrile: ethanol in a ratio of 80: 15: 5 (v/v/v) on a monolithic column at a flow rate of 1.5 mL min⁻¹. The detection potential was 1.2 V versus Ag/AgCl using a BDD electrode.

To obtain the optimal on-line SPE-HPLC-EC conditions, the ratio of methanol to mobile phase for the eluent was 100:0, the flow rate of sample loading and elution was 10 µL s⁻¹, and the eluate zone was 20-24 s. From the validation of this method, the linearity was found to be in the range of 0.01-8 µg mL⁻¹ for SG, SDZ, SMZ, SMM, and SMX, and 0.1-8 µg mL⁻¹ for SDM and SQ. The correlation coefficient of the seven SAs were all greater than 0.99. The LOD and LOQ of this method were in the range of 1.2-11.2 ng mL⁻¹ and 4.0-33.6 ng mL⁻¹, respectively. The recoveries of the sulfonamides in spiked shrimp samples at 2, 4, and 6 µg g⁻¹ were in the range of 74.7 to 110.5 %, with %RSD of intra-day recovery between 0.0 and 13.7 % and %RSD of inter-day recovery between 2.2 and 25.0 %. The percentage recoveries and %RSDs of the proposed method were acceptable according to AOAC International.

This method was compared with HPLC-MS analysis from the Laboratory Center for Food and Agricultural Products Company Limited (LCFA). The proposed method could reduce sample preparation time and reagent consumption and also enabled effective preconcentration and clean-up of the sample. The sensitivity obtained for the seven sulfonamides from this method was high. The results showed that this method was simple, rapid, and highly sensitive for the determination of sulfonamides.

5.2 Suggestion for Further Work

In this work, the on-line SPE-HPLC-EC method was successfully applied to the determination of sulfonamides in shrimp. Furthermore, this method can be applied to the analysis of sulfonamides in other samples, such as animal feed, meat, and milk. In addition, the determination of other antibiotics, such as tetracycline, nitrofurans, and chloramphenicol could also be envisioned.

REFERENCES

- [1] Gehring, T. A., Griffin, B., Williams, R., Geiseker, C., Rushing, L. G., and Siitonen, P. H. Multiresidue determination of sulfonamides in edible catfish, shirmp and salmon tissues by high-performance liquid chromatography with postcolumn derivatization and fluorescence detection. **Journal of Chromatography B** 840 (2006): 132-138.
- [2] Fang, G., He, J., and Wang, S. Multiwalled carbon nanotubes as sorbent for on-line coupling of solid-phase extraction to high-performance liquid chromatography for simultaneous determination of 10 sulfonamides in eggs and pork. **Journal of Chromatography A** 1127 (2006): 12-17.
- [3] Yang, R. F., Shi, Z. G., and Feng, Y. Q. Study on separation of sulfonamides by capillary high-performance liquid chromatography and electrochromatography. **Acta Pharmacologica Sinica** 38 (2003): 129-132.
- [4] Maudens, K. E., and Lambert, W. E. Quantitative analysis of twelve sulfonamides in honey after acidic hydrolysis by high-performance liquid chromatography with post-column derivatization and fluorescence detection. **Journal of Chromatography A** 1047 (2004): 85-92.
- [5] Commission of the European Community, **The rules governing medical products in the European Community IV**. Brussels: 1991.
- [6] You, T., Yang, X., and Wang, E. Determination of sulfadiazine and sulfamethoxazole by capillary electrophoresis with end-column electrochemical detection. **The Analyst** 123 (1998): 2357-2360.

- [7] Fuh, M.S., and Chu, S. Quantitative determination of sulfonamide in meat by solid-phase extraction and capillary electrophoresis. **Analytica Chimica Acta** 499 (2003): 215-221.
- [8] Wang, X., Li, K., Shi, D., et al. Development of an immunochromatographic lateral-flow test strip for rapid detection of sulfonamides in eggs and chicken muscles. **Journal of Agricultural and Food Chemistry** 55 (2007): 2072-2078.
- [9] Chang, H., Hu, J., Asami, M., and Kunikane, S. Simultaneous analysis of 16 sulfonamide and trimethoprim antibiotics in environmental waters by liquid chromatography-electrospray tandem mass spectrometry. **Journal of Chromatography A** 1190 (2008): 390-393.
- [10] McClure, E. L., and Wong, C. S. Solid phase microextraction of macrolide, trimethoprim, and sulfonamide antibiotics in wastewaters. **Journal of Chromatography A** 1169 (2007): 53-62.
- [11] Sheridan, R., Policastro, B., Thomas, S., and Rice, D. Analysis an occurrence of 14 sulfonamide antibacterials and chloramphenicol in honey by solid-phase extraction followed by LC/MS/MS analysis. **Journal of Agricultural and Food Chemistry** 56 (2008): 3509-3516.
- [12] Koesukwiwat, U., Jayanta, S., and Leepipatpiboon, N. Solid-phase extraction for multiresidue determination of sulfonamides, tetracyclines, and pyrimethamine in Bovine's milk. **Journal of Chromatography A** 1149 (2007): 102-111.
- [13] Díaz-Cruz, M. S., García-Galán, M. J., and Barceló, D. Highly sensitive simultaneous determination of sulfonamide antibiotics and one metabolite in environmental waters by liquid chromatography-quadrupole linear ion trap-mass spectrometry. **Journal of Chromatography A** 1193 (2008): 50-59.
- [14] Li, H., Kijak, P. J., Turnipseed, S. B., and Cui, W. Analysis of veterinary drug residues in shrimp: A multi-class method by liquid chromatography-quadrupole ion trap mass spectrometry. **Journal of Chromatography B** 836 (2006): 22-38.

- [15] Ye, Z. Q., Weinberg, H. S., and Meyer, M. T. Trace analysis of trimethoprim and sulfonamide, macrolide, quinolone, and tetracycline antibiotics in chlorinated drinking water using liquid chromatography electrospray tandem mass spectrometry. **Analytical Chemistry** 79 (2007): 1135-1144.
- [16] Choi, K., Kim, S., Kim, C., and Kim, S. Determination of antibiotic compounds in water by on-line SPE-LC/MSD. **Chemosphere** 66 (2007): 977-984.
- [17] Furusawa, N. Rapid high-performance liquid chromatographic determining technique of sulfamonomethoxine, sulfadimethoxine, and sulfaquinoxaline in eggs without use of organic solvents. **Analytica Chimica Acta** 481 (2003): 255-259.
- [18] Granja, R. M., Niño, A. M., Rabone, F., and Salerno, A. G. A reliable high-performance liquid chromatography with ultraviolet detection for the determination of sulfonamides in honey. **Analytica Chimica Acta** 613 (2008): 116-119.
- [19] Gratacós-Cubarsí, M., Castellari, M., Valero, A., and García-Regueiro, J. A. A simplified LC-DAD method with an RP-C12 column for routine monitoring of three sulfonamides in edible calf and pig tissue. **Analytical and Bioanalytical Chemistry** 385 (2006): 1218-1224.
- [20] He, J., Wang, S., Fang, G., Zhu, H., and Zhang, Y. Molecularly imprinted polymer online solid-phase extraction coupled with high-performance liquid chromatography-UV for the determination of three Sulfonamides in pork and chicken. **Journal of Agricultural and Food Chemistry** 56 (2008): 2919-2925.
- [21] Roybal, J. E., Pfenning, A. P., Turnipseed, S. B., Gonzales, S. A. Application of size-exclusion chromatography to the analysis of shrimp for sulfonamide residues. **Analytica Chimica Acta** 483 (2003): 147-152.
- [22] Wen, Y., Zhang, M., Zhao, Q., and Feng, Y.Q. Monitoring of five sulfonamide antibacterial residues in milk by in-tube solid-phase microextraction coupled to high-performance liquid chromatography. **Journal of Agricultural and Food Chemistry** 53 (2005): 8468-8473.

- [23] Niu, H., Cai, Y., Shi, Y., et al. Evaluation of carbon nanotubes as a solid-phase extraction adsorbent for the extraction of cephalosporins antibiotics, sulfonamides and phenolic compounds from aqueous solution. **Analytica Chimica Acta** 594 (2007): 81-92.
- [24] Roudaut, B., and Garnier, M. Sulphonamide residues in eggs following drugadministration via the drinking water. **Food Additives & Contaminants: Part A** 19 (2002): 373 - 378.
- [25] Maudens, K.E. G. Zhang, W.E. Lambert, Quantitative analysis of twelve sulfonamides in honey after acidic hydrolysis by high-performance liquid chromatography with post-column derivatization and fluorescence detection. **Journal of Chromatography A** 1047 (2004): 85-92.
- [26] Preechaworapun, A., Chuanuwatanakul, S., Einaga, Y., Grudpan, K., Motomizu, S., and Chailapakul, O. Electroanalysis of sulfonamides by flow injection system/high-performance liquid chromatography coupled with amperometric detection using boron-doped diamond electrode. **Talanta** 68 (2006): 1726-1731.
- [27] Pereira, A. V., and Cass, Q. B. High-performance liquid chromatography method for the simultaneous determination of sulfamethoxazole and trimethoprim in bovine milk using an on-line clean-up column **Journal of Chromatography B** 826 (2005): 139-146.
- [28] Oliveira, R. V., Pietro, A. C. D., and Cass, Q. B. Quantification of cephalexin as residue levels in bovine milk by high-performance liquid chromatography with on-line sample cleanup. **Talanta** 71 (2007): 1233-1238.
- [29] Oliferova, L., Statkus, M., Tsysin, G., and Zolotov, Y. On-line solid-phase extraction and high performance liquid chromatography determination of polycyclic aromatic hydrocarbons in water using polytetrafluoroethylene capillary. **Talanta** 72 (2007): 1386-1391.
- [30] Yamamoto, E., Takakuwa, S., Kato, T., and Asakawa, N. Sensitive determination of aspirin and its metabolites in plasma by LC-UV using on-line solid-phase extraction with methylcellulose-immobilized anion-exchange restricted access media. **Journal of Chromatography B** 846 (2007): 132-138.

- [31] Tasso, L., and Costa, T. D. High performance liquid chromatography for quantification of gatifloxacin in rat plasma following automated on-line solid phase extraction. **Journal of Pharmaceutical and Biomedical Analysis** 44 (2007): 205-210.
- [32] Liang, H. D., Hua, D. M., and Yan, X. P. Cigarette filter as sorbent for on-line coupling of solid-phase extraction to high-performance liquid chromatography for determination of polycyclic aromatic hydrocarbons in water. **Journal of Chromatography A** 1101 (2006): 9-14.
- [33] Rao, T. N., Sarada, B. V., Tryk, D. A., Fujishima, A. Electroanalytical study of sulfa drugs at diamond electrodes and their determination by HPLC with amperometric detection. **Journal of Electroanalytical Chemistry** 491 (2000): 175-181.
- [34] Economou, A. Sequential-injection analysis (SIA): A useful tool for on-line sample-handling and pre-treatment. **Trends in Analytical Chemistry** 24 (2005): 416-425.
- [35] Ruzicka, J., and Hansen, E.H. Flow injection analyses: Part I. A new concept of fast continuous flow analysis. **Analytica Chimica Acta** 78 (1975): 145-157.
- [36] Stewart, K. K., Beecher, G. R., and Hare, P.E. Rapid analysis of discrete samples: The use of nonsegmented, continuous flow. **Analytical Biochemistry** 70 (1976): 167-173.
- [37] Perez-Olmos, R., Soto, J. C., Zarate, N., Araujo, A. N., and Montenegro, M. C. B. S. M. Sequential injection analysis using electrochemical detection: A review. **Analytica Chimica Acta** 554 (2005): 1-16.
- [38] Barnett, N. W., Lenehan, C. E., and Lewis, S.W. Sequential injection analysis: an alternative approach to process analytical chemistry. **Trends in Analytical Chemistry** 18 (1999): 346-353.
- [39] Ruzicka, J., and Marshall, G. D. Sequential injection: a new concept for chemical sensors, process analysis and laboratory assays. **Analytica Chimica Acta** 237 (1990): 329-343.
- [40] Marshall, G., Wolcott, D., and Olson, D. Zone fluidics in flow analysis: potentialities and applications. **Analytica Chimica Acta** 499 (2003): 29-40.

- [41] Skoog, D. A., West, D. M., and Holler, F. J. **Fundamentals of Analytical Chemistry**. 7th Edition. New York, USA: Saunders College Publishing 1996.
- [42] Harvey, D. **Modern Analytical Chemistry**. USA: The McGraw-Hill, 1976.
- [43] Christian, G. D., and O'Reilly, J. E. **Instrument Analysis**. 2nd Edition: Allyn and Eacon, Inc, 1978.
- [44] Poole, F. C. **The essence of chromatography**. Danvers, USA: Clearance center, Inc., 2003.
- [45] Bard, A. J., and Faulkner, L. R. **Electrochemical Methods: Fundamentals and Applications**. 2nd Edition: John Wiley and Sons, New York, 2001.
- [46] Skoog, D. A., Holler, F. J., and Nieman, T. A. **Principles of Instrument Analysis**. New York, USA: Harcourt Brace College Publishers, 1998.
- [47] Braun, R.D. **Introduction to Instrumental Analysis**. Singapore: McGraw-Hill Book, 1987.
- [48] Sawyer, D. T., Sobkowiak, A., and Roberts, J. L. **Electrochemistry for Chemists**. 2nd Edition. New York: Wiley Interscience, 1995.
- [49] Settle, F. A. **Handbook of Instrumental Techniques for Analytical Chemistry**. New Jersey: Prentice Hall, 1997.
- [50] Thomas, F. G., and Henze, G. **Introduction to Voltammetric Analysis**. Collingwood, Australia: CSIRO Publishing 2001.
- [51] Iland, P., Ewart, A., and Sitters, J. **Techniques for Chemical Analysis and Stability Tests of Grape Juice and Wine**. South Australia: Patrick Iland Wine Promotions, 1993.
- [52] Buchberger, W. W. Detection techniques in ion analysis: what are our choices? **Journal of Chromatography A** 884 (2000): 3-22.
- [53] Trojanowicz, M. **Flow Injection Analysis: Instrumentation and Applications**. Singapore: World Scientific, 2000.
- [54] Fujishima, A., Einaga, Y., Rao, T. N., and Tryk, D. A. **Diamond electrochemistry**. Tokyo: Elsevier-BKC, 2004.
- [55] Zoski, C. G. **Hand book of electrochemistry**.UK: Elsevier, 2006.

- [56] Xu, J. S., Granger, M. C., Chen, Q. Y., Strojek, J. W., Lister, T. E., and Swain, G. M. Boron doped-diamond thin-film electrodes. **Analytical Chemistry** 69 (1997): A591-A597.
- [57] Rao, T. N., Fujishima, A., Angus, J. C., Yasuaki, E., and Tryk, D. A. **Diamond electrochemistry**. Amsterdam: Elsevier Science, 2005.
- [58] Kraft, A. Doped Diamond: A Compact Review on a New, Versatile Electrode Material. **International Journal of Electrochemical Science**. 2 (2007): 355-385.
- [59] Plambeck, J. A. **Electroanalytical Chemistry Basic Principles and Applications**. New York, USA: John Wiley, 1982.
- [60] Mitra, S. **Sample Preparation Techniques in Analytical Chemistry**. Canada, USA: John Wiley & Sons, 2003.
- [61] Thurman, E. M., and Mills, M. S. **Solid-Phase Extraction Principles and Practice**. Canada, USA: John Wiley & Sons, 1998.
- [62] Fritz, J. S. **Analytical Solid-Phase Extraction**. Canada, USA: John Wiley & Sons, 1999.
- [63] Simpson, N. J. K. **Solid-Phase Extraction Principles, Techniques, and Applications**. New York, USA: Marcel Dekker, 2000.
- [64] Sangjarusvichai, H., Dungchai, W., Siangproh, W., and Chailapakul, O. Rapid separation and highly sensitive detection methodology for sulfonamides in shrimp using a monolithic column coupled with BDD amperometric detection. **Talanta** 79 (2009): 1036-1041.

APPENDIX

APPENDIX

Precision and Accuracy

Table A1 Acceptable RSD values according to AOAC International

Analyte %	Analyte ratio	Unit	RSD (%)
100	1	100%	1.3
10	10-1	10%	2.8
1	10-2	1%	2.7
0.1	10-3	0.1%	3.7
0.01	10-4	100 ppm	5.3
0.001	10-5	10 ppm	7.3
0.0001	10-6	1 ppm	11
0.00001	10-7	100 ppb	15
0.000001	10-8	10 ppb	21
0.0000001	10-9	1 ppb	30

Table A2 Acceptable recovery percentages as a function of the analyte concentration

Analyte %	Analyte ratio	Unit	Mean recovery (%)
100	1	100%	98-102
10	10-1	10%	98-102
1	10-2	1%	97-103
0.1	10-3	0.1%	95-105
0.01	10-4	100 ppm	90-107
0.001	10-5	10 ppm	80-110
0.0001	10-6	1 ppm	80-110
0.00001	10-7	100 ppb	80-110
0.000001	10-8	10 ppb	60-115
0.0000001	10-9	1 ppb	40-120

